Genetic dissection of the shoot and root ionomes of Brassica napus grown with contrasting phosphate supplies

Original Article

Genetic dissection of the shoot and root ionomes of *Brassica napus* grown with contrasting phosphate supplies

Wei Wang[1,2], Guangda Ding[1,2], Philip J. White[1,2,3], Meng Wang[1], Jun Zou[1], Fangsen Xu[1,2], John P. Hammond[4,5], Lei Shi[1,2,*]

[1]*National Key Laboratory of Crop Genetic Improvement, Huazhong Agricultural University, Wuhan 430070, China*

[2]*Microelement Research Centre, Key Laboratory of Arable Land Conservation (Middle and Lower Reaches of Yangtze River), Ministry of Agriculture and Rural Affairs, Huazhong Agricultural University, Wuhan 430070, China*

[3]*The James Hutton Institute, Invergowrie, Dundee DD2 5DA, UK*

[4]*School of Agriculture, Policy and Development, University of Reading, Reading RG6 6AR, UK*

[5]*Southern Cross Plant Science, Southern Cross University, PO Box 157, Lismore, NSW 2480, Australia*

Running title: Genetic dissection of the shoot and root ionomes of *Brassica napus*

**For correspondence. E-mail leish@mail.hzau.edu.cn*

Background and Aims Mineral elements have many essential and beneficial functions in plants. Phosphorus (P) deficiency can result in changes in the ionomes of plant organs. The aims of this study were to characterize the effects of P supply on the ionomes of shoots and roots, and to identify chromosomal quantitative trait loci (QTLs) for shoot and root ionomic traits, as well as those affecting the partitioning of mineral elements between shoot and root in *Brassica napus* grown with contrasting P supplies.

Methods Shoot and root concentrations of eleven mineral elements (B, Ca, Cu, Fe, K, Mg, Mn, Na, P, S and Zn) were investigated by ICP-OES in a *Brassica napus* double haploid population grown at an optimal (OP) and a low phosphorus supply (LP) in an agar system. Shoot, root and plant contents, and the partitioning of mineral elements between shoot and root were calculated.

Key Results The tissue concentrations of B, Ca, Cu, K, Mg, Mn, Na, P and Zn were reduced by P starvation, while the concentration of Fe was increased by P starvation in the *Bna*TNDH population. A total of 133 and 123 QTLs for shoot and root ionomic traits were identified at OP and LP, respectively. A major QTL cluster on chromosome C07 had a significant effect on shoot Mg and S concentrations at LP and was narrowed down to a 2.1-Mb region using an advanced backcross population.

Conclusions The tissue concentration and partitioning of each mineral element was affected differently by phosphorus starvation. There was a significant difference in mineral element composition between shoots and roots. Identification of the genes underlying these QTLs will enhance our understanding of processes affecting the uptake and partitioning of mineral elements in *Brassica napus*.

Key words: Mineral element, concentration, content, phosphorus, *Brassica napus*, quantitative trait locus.

INTRODUCTION

Mineral elements have many essential and beneficial functions in plants (Grusak *et al.*, 2016). They serve in structural components, such as cell walls and membranes, in energy transduction, in proteins and metabolites, in nucleotides, in the osmotic and electrochemical balance of cellular compartments, in detoxification of the cytoplasm, and in the regulation of biological activities (Baxter, 2009; Grusak *et al.*, 2016). The elemental composition of an organism, or a constituent part, is referred to as its ionome (Lahner *et al.*, 2003; Neugebauer *et al.*, 2018). The ionome of plant tissues often varies depending on both genetic and non-genetic factors, such as environmental conditions and plant development, and on the interactions between these (Ghandilyan *et al.*, 2009*a*; Neugebauer *et al.*, 2018). A lack or excess of a mineral element will limit plant growth, and tissue concentrations of plants must be maintained within an appropriate range (Grusak *et al.*, 2016).

Phosphorus (P) is an essential macronutrient for plant growth and development (Hawkesford *et al.*, 2012). It is present in membranes, as a component of phospholipids, participates in photosynthesis, energy transduction, and primary and secondary metabolism as a component of metabolites, is essential for gene replication and expression as a component of nucleotides, and serves in intracellular signal transduction via phosphorylation reactions (Hawkesford *et al.*, 2012; Grusak *et al.*, 2016). Lack of available P in soils restricts plant growth, delays development, and reduces crop yields (Hawkesford *et al.*, 2012).

The accumulation of mineral elements in plant organs is determined by a series of

processes, including mobilization from the soil, uptake by roots, translocation from root to shoot in the xylem and recirculation within the plant via the phloem (White and Broadley, 2009; White, 2012*a*, *b*). When the supply of an essential mineral element (nutrient) is compromised this can affect the bioavailability, uptake, transport and utilization of other mineral elements (Watanabe *et al.*, 2015; Neugebauer *et al.*, 2018). Hence, P deficiency can result in changes in the ionomes of plant organs. For example, P deficiency in Arabidopsis results in the inhibition of primary root growth and affects Fe homeostasis through modulation of LPR1 and LPR2 ferroxidases, leading to the apoplastic accumulation of Fe^{3+} (Ward *et al.*, 2008; Müller *et al.*, 2015; Balzergue *et al.*, 2017; Gutiérrez-Alanís *et al.*, 2018). In Arabidopsis shoots, P deficiency results in increased As, B, Fe, and Zn concentrations and decreased Co and Cu concentrations (Baxter *et al.*, 2008). In *Brassica napus*, P deficiency results in reduced concentrations of Ca, Fe, Mg, Mn, and Zn in seeds (Ding *et al.*, 2010). An appreciation of the interactions between P nutrition and the accumulation of other mineral elements in plants may help researchers understand the physiological responses of plants to P deficiency better. However, very little is known about the molecular determinants of alterations in the ionome caused by fluctuations in P supply.

The uptake and accumulation of mineral elements in roots and shoots are most likely affected by many genetic factors (Huang and Salt, 2016). Quantitative trait locus (QTL) analysis is a powerful technique to identify chromosomal regions containing genetic factors linked to variation in complex traits (Paran and Zamir, 2003). A large number of QTLs have been detected that affect the acquisition and accumulation of mineral

elements in plant tissues (e.g. Bentsink *et al.*, 2003; Loudet *et al.*, 2003, 2007; Payne *et al.*, 2004; Vreugdenhil *et al.*, 2004; Harada and Leigh, 2006; Waters and Grusak, 2008; Ghandilyan *et al.*, 2009*a, b*; Sánchez-Bermejo *et al.*, 2014; Wang *et al.*, 2019) and a number of genes impacting the plant ionome have been cloned using forward genetics in Arabidopsis (reviewed in Huang and Salt, 2016). In *Brassica rapa*, several QTLs have been discovered that affect seed and leaf phosphate concentrations (Zhao *et al.*, 2008) and leaf Al, Fe, Mg, Mn, Na, P, Sr and Zn concentrations (Wu *et al.*, 2008). In *Brassica oleracea*, QTLs have been identified for shoot Ca and Mg concentrations (Broadley *et al.*, 2008), shoot P concentration (Hammond *et al.*, 2009), and shoot K and Na concentrations (White *et al.*, 2010). In *B. napus*, QTLs influencing shoot B, Ca, Cu, Fe, Mg, P and Zn concentrations (Liu *et al.*, 2009), seed Ca, Cu, Fe, Mg, Mn, P and Zn concentrations (Ding *et al.*, 2010) and seed S concentration (Körber *et al.*, 2016), have been identified.

In addition to traditional linkage mapping using biparental recombinant populations, genome-wide association analysis (GWAS) can be used to uncover the genetic basis of complex traits, including ionomic traits (e.g. Atwell *et al.*, 2010; Yang *et al.*, 2018). More QTLs with a narrower mapping interval can be detected by GWAS using natural populations that contain extensive genetic diversity and have undergone numerous recombination events (Xiao et *al.*, 2017). Bus *et al.* (2014) identified several significant single nucleotide polymorphisms (SNPs) associated with shoot Ca, Cu, Mg, Mn, Na, S and Zn concentrations in *B. napus* through GWAS. Additionally, a number of SNPs and gene expression markers were discovered for leaf nitrate, phosphate and sulfate

concentrations (Koprivova *et al.*, 2014), leaf Ca and Mg concentrations (Alcock *et al.*, 2017), and leaf nitrate, P and K concentrations (Alcock *et al.*, 2018) through associative transcriptomics. Although the identity of the underlying genes remains unknown, these studies have demonstrated the presence of allelic variation affecting the accumulation of mineral elements in Brassicaceae crops.

Brassica napus ($A_nA_nC_nC_n$, ~1130 Mb, $2n=4x=38$) is an allopolyploid crop derived from interspecific crosses between the diploid progenitors, *B. rapa* (A_rA_r, $2n=2x=20$) and *B. oleracea* (C_oC_o, $2n=2x=18$) (Chalhoub *et al.*, 2014). It is the third largest source of vegetable oil globally. However, it is highly susceptible to P deficiency (Duan *et al.*, 2009). To date, few studies have been performed to detect QTLs associated with shoot and root ionomes under the same conditions in any Brassicaceae crop. In the present study, a *B. napus* double haploid (*Bna*TNDH) population derived from a cross between cultivars Tapidor and Ningyou 7 was employed (Qiu *et al.*, 2006). The shoot and root ionomic profiles (B, Ca, Cu, Fe, K, Mg, Mn, Na, P, S and Zn) of 182 genotypes from the *Bna*TNDH population grown in an agar system with an optimal (OP) or a low P supply (LP) were examined. The objectives of the study were (i) to characterize the effects of P supply on the uptake of mineral elements and the ionomes of shoot and root tissues of *B. napus*, (ii) to identify QTLs and QTL clusters associated with shoot and root ionomic traits, as well as those affecting the partitioning of mineral elements between shoot and root tissues, at OP and LP, and (iii) to elucidate differences in the genetic control of shoot and root ionomic traits when plants are grown with contrasting P supplies.

MATERIALS AND METHODS

Plant materials and growing conditions

The *Bna*TNDH mapping population employed consisted of 182 lines generated through anther culture of the F_1 generation of a cross between a European winter-type cultivar Tapidor containing a low glucosinolate concentration (Sharpe and Lydiate, 2003), and Ningyou 7, a Chinese semiwinter-type cultivar with high glucosinolate concentration (Qiu *et al.*, 2006).

To fine map candidate QTLs, an advanced backcross population consisting of 860 BC_4F_1 lines, which were generated with cultivar Tapidor as the recurrent parent and cultivar Ningyou 7 as the donor parent (Zeng, 2011), were employed to confirm and resolve the QTLs identified in the *Bna*TNDH population. Each BC_4F_1 line was self-pollinated to produce the BC_4F_2 population. Genomic DNA of six BC_4F_2 individuals selected randomly from each BC_4F_1 line was bulked in an equal ratio to generate bulk DNA, and these six individuals were further self-pollinated to construct the $BC_4F_{2:3}$ population. These DNA bulks and the genomic DNA of the two parental cultivars were subjected to specific-locus amplified fragment sequencing using an Illumina HiSeq 2500 sequencer with a paired-end pattern.

The root traits and biomass traits of the *Bna*TNDH population and its parents had been screened previously in an agar system both at a phosphate (Pi) concentration of 0.625 mM (an optimal phosphorus supply, OP) and at a Pi concentration of 0 mM (a low phosphorus supply, LP) (Shi *et al.*, 2013). In this study, five $BC_4F_{2:3}$ lines (1757-3, 1856-3, 1856-4, 2292-3 and 2303-4) were screened in the agar system at LP, and

Tapidor and Ningyou 7 at both OP and LP.

Briefly, surface sterilized seeds were sown into vented polystyrene trays (QTray; 240 × 240 × 20 mm; Molecular Devices, Hampshire, UK) containing 300 mL 0.8% (w/v) agar and a modified basal salt mix (Murashige and Skoog, 1962) with either K and Pi added as KH_2PO_4 for OP or with 0.625 mM KCl added to provide K for LP. Seeds were sown 3 cm from the top edge of a tray, with four seeds per line and two lines per tray. Trays were sealed with Nescofilm and placed 10° from vertical in a growth room under a 16-h photoperiod at a constant temperature of 24 °C. Illumination was provided by a bank of 84 100-W cool fluorescent tubes (Philips, Eindhoven, Netherlands), giving a photon flux density between 400 and 700 nm of 80–100 μmol photons m^{-2} s^{-1} at plant height. For each line, 16 seeds were sown across four independent replicates, at both OP and LP. Trays were placed randomly within the growth room.

Phenotypic analyses

Shoots and roots were harvested separately and dried at 80 °C 12 d after sowing. Shoot dry weight (SDW) and root dry weight (RDW) were determined, and total plant dry weight (TDW) was calculated as the sum of SDW and RDW. Prior to analysis, TDW, SDW and RDW were natural logarithm (ln)-transformed to improve the normality and variance of the data. To acquire adjusted line means, the REML (residual maximum likelihood) procedure in GenStat (15^{th} Edition, VSN International Ltd, Hemel Hempstead, UK) was performed using the [($[P]_{ext}$ × Line)] term as a fixed factor and [(Replicate/Run/Plate/Position)] as a random factor.

The mineral element concentrations in shoot and root dry matter were measured using inductively coupled plasma optical emission spectrometry (ICP-OES) (JY Ultima 2; Jobin Yvon Ltd, Stanmore, Middlesex, UK). All the replicate samples for each line were mixed together, oven dried at 80 °C for at least 48 hours and then milled. Approximately 0.1 g dried ground powder was put into a PTFE digestion tube together with 1 ml concentrated nitric acid, closed tightly and processed in a closed vessel acid digestion microwave (MARSXpress; CEM Corporation, Matthews, NC, USA). After cooling, each digest was diluted to a final volume of 10 ml with deionized water. These dilutions were used to measure mineral element concentration by ICP-OES. For each mineral element, shoot content was calculated as the product of shoot concentration and SDW, and root content as the product of root concentration and RDW. Plant mineral element contents were calculated as the sum of shoot mineral element content and root mineral element content. The partitioning of a mineral element to the shoot was calculated as the quotient of shoot mineral element content divided by plant mineral element content (Wu *et al.*, 2015).

QTL mapping and integration of the QTL clusters

The *Bna*TNDH linkage map used in this study was constructed as previously described (Zhang *et al.*, 2016). This map spanned 2077.9 cM in length and contained 1698 SNP markers and 343 original markers on 19 chromosomes, with an average distance of 1.02 cM between adjacent markers. The additive and epistatic QTLs for different traits at both OP and LP were determined using the QTL IciMapping v4.1 (Meng *et al.*, 2015)

using single environment phenotypic values. Briefly, for the additive QTL, the ICIM-ADD mapping method was exploited in the software. The walk speed was 1 cM, and the *P* values for entering variables (PIN) and removing variables (POUT) were set at 0.001 and 0.002, respectively. The epistatic QTLs were identified by the ICIM-EPI mapping method. The walk speed was 5 cM, and PIN and POUT were set at 0.0001 and 0.0002, respectively. The LOD thresholds for the additive QTL and epistatic QTL were set to 2.5 and 5.0 as the default manual input value, respectively. The phenotypic variation explained by each additive QTL or epistatic QTL and the corresponding additive effects were also estimated using the same software.

A QTL cluster was defined as two or more significant QTLs with overlapping confidence intervals. For a QTL cluster, the coincidence of QTLs for two or more traits was considered to be positive if the alleles increasing trait values were from the same parent, while it was considered to be negative if the alleles increasing trait values were from different parents (Coque *et al.*, 2008). QTL meta-analysis was performed using BioMercator v4.2 (Arcade *et al.*, 2004). Meta-analysis computing was based on the position of each input QTL, and on the variance of this position, assessed through confidence interval values. The algorithm developed by Goffinet and Gerber (2000) was employed to perform the analysis.

Confirmation and resolution of the QTL cluster Cl17.1 and prediction of candidate genes

The 860 BC_4F_1 substitution lines of *B. napus*, in which the segments of cultivar Ningyou

7 were introgressed into the genetic background of cultivar Tapidor, were genotyped with 17116 genome-wide markers (InDels and SNPs) produced from SLAF-seq (data not shown). Nine BC_4F_1 lines were screened based on the two flanking markers of the QTL cluster Cl17.1. These lines showed more than 90% genetic similarity to the recurrent parent (Tapidor) and did not harbour any other QTLs containing Ningyou 7 alleles affecting shoot K, Mg and S concentrations at LP. The $BC_4F_{2:3}$ lines derived from these nine BC_4F_1 lines were further genotyped using the five InDel markers located in the region of the QTL cluster Cl17.1. Finally, five $BC_4F_{2:3}$ lines (1757-3, 1856-3, 1856-4, 2292-3 and 2303-4) were identified with whole or part homozygous donor segments of the QTL cluster Cl17.1. The five $BC_4F_{2:3}$ lines were grown at LP in the agar system for 12 d, and the shoot K, Mg and S concentrations of these five lines were measured by ICP-OES. The QTL cluster Cl17.1 was confirmed and resolved from the phenotypes and genotypes of the five $BC_4F_{2:3}$ lines. The resolved QTL cluster Cl17.1 was mapped to the reference genome (cultivar Darmor-*bzh*) based on the physical position of the two flanking markers. The available reference genome of *B. napus* (Chalhoub *et al.*, 2014) and the functional annotation of the Arabidopsis genome (https://www.arabidopsis.org/) were employed for the prediction of putative candidate genes.

RESULTS

Variation and correlation of shoot concentrations of eleven mineral elements among the Bna*TNDH population at OP and LP*

To establish variation in the ionome, a meta-analysis of shoot and root ionomes in the parental lines Tapidor and Ningyou 7 was conducted. Ionome data from shoots and roots of plants grown with a range of external P concentrations in an agar system obtained from this and previous work (Shi *et al.*, 2013) and of plants grown with low and high B concentrations in a hydroponic system (Liu *et al.*, 2009) were analysed. Across these multiple environments, Tapidor had higher shoot B, Cu and P concentrations, but lower shoot K and S concentrations, than Ningyou 7 (Fig. 1A).

Shoot concentrations of Cu, K, Mg and P were reduced by P starvation in both Tapidor and Ningyou 7, while shoot concentrations of Ca and Mn were only reduced by P starvation in Ningyou 7 (Fig. 2A; Supplementary Data Table S1). By contrast, shoot Fe and S concentrations of both cultivars and the shoot Na concentration of Tapidor were increased by P starvation.

The mean shoot B, Fe, Na, S and Zn concentrations of the *Bna*TNDH population were greater at LP than at OP, but the mean shoot Ca, Cu, K, Mg and P concentrations were lower at LP than at OP (Fig. 3; Supplementary Data Table S1). Shoot Ca and Mn concentrations of the *Bna*TNDH population had the highest correlation coefficients among the eleven mineral elements studied at both OP ($r = 0.75$) and at LP ($r = 0.84$; Table 1). Among the genotypes of the *Bna*TNDH population there were significant positive correlations in shoot concentrations between OP and LP for all eleven mineral

elements studied, except for Zn (Table 1).

Variation and correlation of root concentrations of eleven mineral elements among the Bna*TNDH population at OP and LP*

Tapidor had significantly higher root K and Mg concentrations, but a lower root Na concentration than Ningyou 7 across the multiple growing environments (Fig. 1B). The root P concentration in both Tapidor and Ningyou 7 was significantly reduced by P starvation (Fig. 2B; Supplementary Data Table S1). Root B, Fe, K, Mn and Na concentrations were reduced only in cultivar Tapidor and root Mg concentration was reduced only in cultivar Ningyou 7 by P starvation. By contrast, root Cu and S concentrations of both cultivars were increased by P starvation.

The mean root Cu and S concentrations of the *Bna*TNDH population were greater at LP than at OP (Fig. 3; Supplementary Data Table S1). By contrast, root B, K, Mg, Mn, Na and P concentrations were lower at LP than at OP. Root Ca and Mn concentrations had the highest correlation coefficients among the eleven mineral elements at both OP ($r = 0.70$) and LP ($r = 0.76$; Table 1). There were significant positive correlations in root concentrations between OP and LP for all eleven mineral elements studied in the *Bna*TNDH population, except for Cu, P and Zn (Table 1). Generally, stronger correlations were detected between shoot concentrations of mineral elements and between root concentrations of mineral elements at LP than at OP (Table 1).

Difference in concentrations of eleven mineral elements between shoot and root among

the Bna*TNDH population at OP and LP*

Shoot mineral element concentrations of the *Bna*TNDH population clustered separately from their root mineral element concentrations in a PCA (principal component analysis) biplot at both OP and LP (Fig. 4). The first component accounted for 58.3% and 60.3% of the total variation at OP and LP, respectively, and mainly represented the contrast between B+Ca+Mg+Mn+Na+P and Fe at both OP and LP. Interestingly, Cu was loaded positively onto PC1 at OP, but negatively onto PC1 at LP. The second component, accounting for 10.6% and 14.7% of the total variation at OP and LP, respectively, mainly represented K and Zn at both OP and LP. In addition, S was loaded in nearly equal proportion between PC1 and PC2 at both OP and LP.

Variation and correlation of shoot and root contents of eleven mineral elements among the Bna*TNDH population at OP and LP*

Tapidor had lower shoot contents than Ningyou 7 of all eleven mineral elements studied at both OP and LP, except for Cu at LP and Fe at OP (Supplementary Data Table S2). The mean shoot Fe content of the *Bna*TNDH population was higher at LP than at OP (Fig. 3; Supplementary Data Table S2). By contrast, the mean shoot Ca, Cu, K, Mg, Mn and P contents of the *Bna*TNDH population were lower at LP than at OP.

Tapidor had lower root contents of all the eleven mineral elements studied than Ningyou 7 at both OP and LP, except for Cu at LP (Supplementary Data Table S2). The mean root Cu content in the *Bna*TNDH population was higher at LP than at OP, while the mean root B, Ca, Fe, K, Mg, Mn, Na, P and Zn contents were lower at LP than at OP (Fig. 3; Supplementary Data Table S2). Significant correlations were observed

among shoot and root contents of all the eleven mineral elements in the *Bna*TNDH population at both OP and LP (Supplementary Data Table S3). Significant positive correlations were also observed in shoot and root contents of all the eleven mineral elements between OP and LP (Supplementary Data Table S3).

Variation and correlations of whole plant mineral element contents among the Bna*TNDH population at OP and LP*

Tapidor had lower plant contents of all mineral elements than Ningyou 7 at both OP and LP, except for Cu at LP (Supplementary Data Table S4). The mean plant Fe content of the *Bna*TNDH population was greater at LP than at OP, while the mean plant B, Ca, Cu, K, Mg, Mn, Na, P and Zn contents were lower at LP than at OP (Fig. 3; Supplementary Data Table S4).

Significant positive correlations among the plant contents of all eleven mineral elements were observed at both OP and LP in the *Bna*TNDH population, with the lowest significant correlation coefficient (r = 0.28) between plant Fe and P content at LP and the highest correlation coefficient (r = 0.95) between plant Ca and Mn content at both OP and LP (Table 2). The plant contents of all the eleven mineral elements studied were significantly positively correlated between OP and LP in the *Bna*TNDH population (Table 2).

Variation and correlations in partitioning of eleven mineral elements to the shoot among the Bna*TNDH population at OP and LP*

Tapidor and Ningyou 7 differed less than 5% in their partitioning of individual mineral elements to the shoot at OP and LP, except for Fe (11.1% at OP and 23.6% at LP) (Supplementary Data Table S4). The mean partitioning to the shoot of all eleven mineral elements studied in the *Bna*TNDH population was greater than 80% at both OP and LP, with the exception of Cu at LP (66.7%) and Fe at OP (19.9%) and LP (36.6%). The partitioning of B, Fe, Na and Zn to the shoot in the *Bna*TNDH population was greater at LP than at OP (Fig. 3; Supplementary Data Table S4). In contrast, partitioning of Ca, Cu, K and P to the shoot was less at LP than at OP.

There were significant positive correlations in the partitioning of all the eleven mineral elements studied at both OP and LP, except between Cu and Ca, Fe, K, Mg, Mn and Na at OP (Table 2). The partitioning of Ca to the shoot was highly correlated with the partitioning of Mn to the shoot in the *Bna*TNDH population at both OP ($r = 0.86$) and LP ($r = 0.87$), suggesting that the distribution of these two mineral elements within the plant might be controlled by similar transport processes. It is noteworthy that, for example, neither Ca nor Mn are readily mobile in the phloem (White, 2012b; Grusak *et al.*, 2016). The partitioning to the shoot of all eleven mineral elements studied in the *Bna*TNDH population were significantly positively correlated between OP and LP (Table 2). However, Cu and Fe partitioning to the shoot at OP had a relatively weak correlation with their partitioning at LP, suggesting that there might be a difference in the control of the partitioning of these two mineral elements to the shoot between OP and LP.

QTLs and epistatic interactions for mineral element concentrations, contents, and partitioning to the shoot at OP and LP

Approximately normal distributions and transgressive segregations were observed for all the ionomic traits studied in the *Bna*TNDH population at both OP and LP (Supplementary Data Tables S1, S2 and S4; Supplementary Data Figs. S1–S6), indicating a quantitative inheritance pattern suitable for QTL identification. A total of 41 QTLs distributed across twelve chromosomes were associated with shoot concentrations of the eleven mineral elements at OP and LP, explaining 1.4–19.3% of the phenotypic variation (Table 3). Among these QTLs, CaconcLPS-A07 for shoot Ca concentration at LP, KconcOPS-C08a for shoot K concentration at OP, and SconcOPS-A09 and SconcOPS-C07 for shoot S concentration at OP accounted for 18.0%, 17.1%, 19.3% and 19.3% of the phenotypic variation for these traits, respectively. For both shoot Ca and Mn concentrations, the associated QTLs identified at OP and LP were closely linked on chromosome A07.

A total of 34 QTLs for root concentrations of the eleven mineral elements at OP and LP explained 4.6–23.1% of the phenotypic variation, and were located on 15 of the 19 chromosomes of *B. napus* (Table 3). Among these QTLs, SconcOPR-A04 and SconcOPR-C01 for root S concentration at OP and SconcLPR-A04a for root S concentration at LP accounted for 19.2%, 20.5% and 23.1% of the phenotypic variation, respectively. In addition, the QTLs for the shoot and root S concentrations were co-located on chromosome A09 at OP.

In total, 52 QTLs on seven chromosomes were associated with shoot contents of the

eleven mineral elements at OP and LP, which accounted for 0.7–23.0% of the phenotypic variation (Table 3). Among these QTLs, CucontOPS-A03 for shoot Cu contents and PcontOPS-A02 for shoot P contents at OP explained 16.6% and 23.0% of the phenotypic variation, respectively. There was a close linkage relationship between the QTLs for the shoot contents of five mineral elements (B, Ca, Mn, Na and Zn) identified at OP and at LP on chromosome A03, which may be due to the close linkage relationship between the QTLs identified for SDW at OP and at LP (Table 3). A close linkage relationship was also observed between the QTLs detected for the shoot contents of four mineral elements (Ca, K, Mg and S) at OP and LP on chromosome A04. In addition, a stable QTL affecting shoot K content was detected on chromosome A03 at OP and LP.

Twenty-nine QTLs across ten chromosomes for root contents of the eleven mineral elements at OP and LP explained 4.9–14.5% of the phenotypic variation (Table 3). Moreover, the QTLs for the shoot and root contents of five mineral elements (Ca, K, Mn, Na and Zn) were co-located on chromosome A03 at LP, and QTLs for the shoot and root S contents were co-located on chromosome C04 at OP.

A total of 46 QTLs distributed across eight chromosomes were associated with plant contents of the eleven mineral elements at OP and LP, explaining 5.1–16.0% of the phenotypic variation (Table 3). One QTL, CucontOPP-A03 for plant Cu content at OP, accounted for 16.0% of the phenotypic variation. The QTLs for the plant contents of B, Ca, K, Mn, Na and S identified at OP and at LP had close linkage relationships.

A total of 54 significant QTLs, including 33 at OP and 21 at LP, were detected for

partitioning of the eleven mineral elements to the shoot (Table 3). These QTLs were located on 15 chromosomes, explaining 4.0–24.9% of the phenotypic variation. The QTLs for the partitioning of Mg to the shoot at OP and LP and those for the partitioning of S to the shoot at OP and LP were closely linked on chromosomes C04 and A04, respectively. Moreover, a QTL for the partitioning of Ca to the shoot on chromosome C09 was identified at both OP and LP (Table 3).

A total of 54 epistatic interactions, including 31 at OP and 23 at LP, were detected for shoot and root concentrations, shoot, root and plant contents, and partitioning to the shoot of the eleven mineral elements in the *Bna*TNDH population (Fig. 5; Table 4). There were 25 epistatic interactions in the A genome (A01–A10), 13 in the C genome (C01–C09), and 16 between the two genomes of *B. napus* (Table 4). The individual phenotypic contributions of these epistatic interactions for different traits ranged from 6.8% to 24.4%, and three pairs of them explained more than 20.0% of the phenotypic variation. None of these epistatic interactions involved any additive QTL except for one pair showing a QTL/non-QTL interaction for root Mn concentration at OP (Supplementary Data Table S5).

A pleiotropic epistatic interaction affecting root B, K and Mn contents at OP was identified on chromosome A10, and another one affecting root B, K, Mn and Zn contents at OP was found on chromosome C09 (Fig. 5A). A pleiotropic epistatic interaction for shoot K content and plant K and Na contents at LP was detected between chromosome A08 and C05, and another one for root B content and plant Mn content at LP was discovered between chromosome A03 and A08 (Fig. 5B). Although an epistatic

interaction was detected for TDW at both OP and LP, these two pairs did not overlap with any of the previously identified 54 epistatic interactions (Fig. 5), implying that these 54 epistatic interactions may affect the uptake and transport of different mineral elements. All these epistatic interactions for the same trait were not detected consistently across OP and LP (Table 4).

The number of additive QTLs and epistatic interactions varied from zero to five and from zero to four, respectively (Supplementary Data Table S5). The additive QTLs and epistatic interactions accounted for 0–51.9% and 0–48.7% of the total phenotypic variation, respectively. The total phenotypic variation explained by the additive QTL was more than 50% for shoot and root S concentrations at OP, which could provide targets for *B. napus* breeding programmes. The presence of additive QTLs and epistatic interactions with positive and negative effects could provide the genetic basis for the transgressive segregation of the traits studied.

QTL clusters for shoot and root concentrations, shoot, root and plant contents, and partitioning to the shoot of eleven mineral elements at OP and LP

A total of 49 QTL clusters were identified across twelve chromosomes in a meta-analysis (Fig. 6; Supplementary Data Table S6). There were 17, 14 and 18 QTL clusters detected at OP, LP, and both OP and LP, respectively. Six QTL clusters (Cl2.3, Cl3.3, Cl3.4, Cl4.2, Cl4.3 and Cl19.2) were associated with more than three traits impacting mineral element composition (Supplementary Data Table S6). Among these QTL clusters, four QTL clusters (Cl2.3, Cl3.3, Cl3.4 and Cl4.2) overlapped with QTLs for

biomass traits, while two QTL clusters Cl4.3 and Cl19.2 were not associated with biomass traits. Cl4.3 was associated with shoot B, Ca, K, Mg, Mn, Na, S and Zn contents, plant Ca, K, Mg, Mn, Na and S contents, and the partitioning of B to the shoot at LP. The alleles with positive effects in this QTL cluster were contributed by Ningyou 7. Cl19.2 was associated with root Zn content and plant Ca, Mn and Na contents at OP. The alleles with positive effects in this QTL cluster were contributed by Tapidor.

Confirmation and refinement of the QTL cluster Cl17.1 associated with shoot K, Mg, and S concentrations at LP

Given the consistent difference in the shoot K and S concentrations between Tapidor and Ningyou 7 across multiple environments (Fig. 1A), the QTL cluster Cl17.1 may be a robust locus. The presence of the QTL cluster Cl17.1 was confirmed and resolved further using substitution lines. Shoot K, Mg and S concentrations of the five $BC_4F_{2:3}$ lines (1757-3, 1856-3, 1856-4, 2292-3 and 2303-4) and the two parental lines were determined at LP in the agar system (Fig. 7). There was no significant difference in shoot K concentration between Tapidor and any of the five $BC_4F_{2:3}$ lines, although an obvious difference in this trait was observed between the cultivars Tapidor and Ningyou 7 (Fig. 7A). This suggests that the QTL cluster Cl17.1 had only a minor effect on shoot K concentration, in line with the small fraction of phenotypic variation (3.6%) explained by the QTL KconcLPS-C07 (Table 3). In contrast, all five $BC_4F_{2:3}$ lines had significantly higher shoot Mg concentrations than Tapidor, although there was no significant difference in this trait between the cultivars Tapidor and Ningyou 7 (Fig.

7B). In addition, four of the five $BC_4F_{2:3}$ lines had significantly higher shoot S concentrations than Tapidor, the exception being line 2303-4 (Fig. 7C). The allele from Ningyou 7 within the QTL cluster Cl17.1 had a positive effect on both shoot Mg and S concentrations in all five $BC_4F_{2:3}$ lines. Thus, it was consistent with the positive contribution of the Ningyou 7 allele to the trait value in the *Bna*TNDH population (Table 3). The QTL cluster Cl17.1 was narrowed down to 28.5–30.6 Mb on chromosome C07 using knowledge of the introgression regions of these five lines (Fig. 7D).

DISCUSSION

The uptake and partitioning to the shoot of eleven mineral elements and their QTLs were differentially influenced by P starvation in B. napus

The application of high-throughput elemental analysis has facilitated the quantitative and simultaneous measurement of the elemental composition of living organisms (Salt *et al.*, 2008). In this study, the biomass and concentrations of eleven mineral elements (B, Ca, Cu, Fe, K, Mg, Mn, Na, P, S and Zn) in the shoot and root were investigated in the *Bna*TNDH population grown at OP and LP (Figs. 1–3). Direct interactions between cations and anions in their uptake are rare since they occur through different transporters, but the uptake of one mineral element can affect the uptake of another indirectly through effects on the membrane potential, the proton electrochemical gradient or via feedback regulation through plant growth, metabolism or cellular homeostasis (White, 2012*a*). Thus, the decrease in the plant content of Ca, Cu, K, Mg,

Mn, Na and Zn in P-deficient *B. napus* (Fig. 3; Supplementary Data Table S4) might be a consequence of reduced growth, as was reported previously in *B. napus* grown in a hydroponics system (Maillard *et al.*, 2016). Traits affecting root morphology and anatomy play a key role in the acquisition of mineral elements by plants (White *et al.*, 2013) and a significant positive correlation between leaf Ca (and Zn) concentrations and lateral root density (LRD) was observed in field trials with *B. napus* (Thomas *et al.*, 2016*a*, *b*). In the experiments reported here, the concentrations of mineral elements in the shoot had no correlations, or significant negative correlations, with LRD, but shoot B, Ca, Cu, Fe, K, Mg, Mn, Na, P and Zn concentrations had significant positive correlations with PRL and/or LRL at OP and LP (Supplementary Data Table S7), suggesting that greater root length might improve nutrient acquisition in an agar system with a homogeneous nutrient availability. By contrast, the shoot Fe concentration was greater in plants at LP than at OP (Fig. 3; Supplementary Data Table S4), possibly because P and Fe can precipitate together when Pi concentrations are high, which results in reduced Fe availability (Dalton *et al.*, 1983; Ward *et al.*, 2008).

In addition to the uptake of mineral elements by roots, the translocation of mineral elements from the root to the shoot in the xylem and their recirculation within the plant via the phloem affect the accumulation of mineral elements in the shoot. The mean partitioning of all eleven mineral elements to the shoot was more than 80% in the *Bna*TNDH population grown at OP, except for Fe (Supplementary Data Table S4), suggesting that mineral nutrients were preferentially partitioned to the shoot to maintain plant growth and development. The rather low partitioning of Fe to the shoot (19.9%)

led to a relatively low mean shoot Fe concentration (92.7 μg g^{-1} DW) and a relatively high mean root Fe concentration (2013 μg g^{-1} DW) in the *Bna*TNDH population at OP (Supplementary Data Table S1). Similarly, mean rosette Fe concentration (39 μg g^{-1} DW) was much lower than mean root Fe concentration (1680 μg g^{-1} DW) in an Arabidopsis RIL population (Ghandilyan *et al.*, 2009*b*), and root Fe concentrations were greater than shoot Fe concentrations in *B. oleracea* genotypes, which was exacerbated by greater P supply (Pongrac *et al.*, 2020). It was also found that Fe concentrations in the roots of many Brazilian tree species were greater than their shoot Fe concentrations when grown hydroponically in a complete nutrient solution (Neugebauer *et al.*, 2019). It may be argued that the large amounts of Fe stored in roots are necessary to sustain the normal growth of roots, serve as a Fe reserve for periods of reduced Fe availability, or protect the shoot from Fe toxicity.

The partitioning to the shoot of each of the eleven mineral elements was affected differently by P starvation in *B. napus* (Fig. 3; Supplementary Data Table S4). The partitioning of Cu and Fe to the shoot were most strongly influenced by P starvation. The partitioning of Cu to the shoot decreased by 23% and the partitioning of Fe to the shoot increased by 84% at LP (Supplementary Data Table S4). Iron is transported mainly in the form of Fe^{3+} citrate in the xylem (Welch, 1995; von Wirén *et al.*, 1999). In Arabidopsis, AtFRD3, a member of the multidrug and toxin efflux (MATE) transporter family, is expressed in the root pericycle and appears to be involved in loading citrate into the xylem (Durrett *et al.*, 2007; Puig *et al.*, 2007). *BnaA05g29700D* and *BnaC05g44030D* are the homologous genes of *AtFRD3* in *B. napus*. The expression

of both these genes was significantly induced in roots of P-deficient plants (Li *et al.*, 2019), which might result in greater Fe translocation from roots to shoots and account for an increased Fe partitioning to the shoot in *B. napus* at LP. The Arabidopsis P-type ATPase HMA5 (AtHMA5) is involved in loading Cu into the xylem for root-to-shoot translocation and/or Cu detoxification in the root (Andrés-Colás *et al.*, 2006; Kobayashi *et al.*, 2008). The expression of *BnaA10g06240D* (a homologous gene of *AtHMA5* in *B. napus*) was reduced in roots of *B. napus* plants at LP (Li *et al.*, 2019), which might account for a significantly reduced Cu partitioning to the shoot at LP.

A total of 133 and 123 QTLs for shoot and root ionomic traits were identified at OP and LP, respectively. For each ionomic trait, most of the QTLs identified at OP differed from the QTLs detected at LP in the present study. Similar observations were made by Ding *et al.* (2010) that the QTLs affecting seed mineral element concentrations in *B. napus* in P-deficient plants differed from those affecting seed mineral element concentrations in P-replete plants. Moreover, different QTLs affected shoot mineral element concentrations in B-deficient and B-replete *B. napus* plants (Liu *et al.*, 2009). Given the large number of solute-specific and non-specific transport proteins in plants (Mäser *et al.*, 2001) and the sophisticated regulation of their activities in response to plant nutritional status, it is perhaps unsurprising that the ionomes of plant organs and QTLs affecting the uptake and partitioning of mineral elements between organs should differ at OP and LP.

Several QTLs for shoot Ca, K and Mg concentrations detected at OP in this study were mapped to the same chromosome of *B. napus* on which a number of SNPs

associated with shoot Ca, K and Mg concentrations were also identified by associative transcriptomics (Alcock *et al.*, 2017, 2018). However, it is difficult to determine whether these QTLs for the same trait were located on the same chromosomal regions because the physical positions of the SNPs detected by Alcock *et al* (2017, 2018) are not available. Further studies should be performed to confirm the stability of these QTLs across different populations and/or environments.

Significant differences in the concentrations of mineral element in shoots and roots and their genetic control

Mean shoot B, Ca, Mg, Mn, Na and P concentrations in the *Bna*TNDH population were greater than those in the root regardless of P supply (Fig. 4; Supplementary Data Table S1). By contrast, root Fe, S and Zn concentrations were greater than those in the shoot at both OP and LP. These observations indicate that mineral element composition is organ specific in plants. In Arabidopsis, higher shoot B, Mg, Mn and Na concentrations, but lower shoot Fe, S and Zn concentrations were also observed at both OP and LP (Ghandilyan *et al.*, 2009*b*; Gruber *et al.*, 2013). The variation in concentrations of mineral elements among different organs might be associated with the specific biological functions of these organs. For example, relatively high Mg and Mn concentrations in the shoot might be important for photosynthetic efficiency (Black *et al.*, 2006; Kering *et al.*, 2009).

In general, the concentrations of mineral elements in shoots had relatively weak correlations with those in the root (Supplementary Data Table S8), as was observed

previously in *B. napus* (Thomas *et al.*, 2016*a*). QTLs associated with shoot and root concentrations of most mineral elements did not overlap although co-located QTLs for shoot and root S concentrations were identified on chromosome A09 at OP. Similarly, a striking difference in QTLs associated with the concentrations of mineral elements in different plant organs (root, rosette and seed) was found in Arabidopsis (Ghandilyan *et al.*, 2009*b*).

QTLs for ionomic traits for different mineral elements mapped to the same locus

Significant positive correlations were observed among many ionomic traits, such as shoot and root concentrations, shoot, root and plant contents, and partitioning to the shoot, of the eleven mineral elements in the *Bna*TNDH population across P treatments (Table 1; Table 2; Supplementary Data Table S3). Correlations among traits for mineral elements could be the result of element-element interactions, but could also result from genetic linkage of the QTLs controlling these traits (Fig. 6; Supplementary Data Table S6). For example, shoot and root concentrations, shoot, root and plant contents, and partitioning of Ca to the shoot were highly correlated with those traits for Mn at both OP and LP (Table 1; Table 2; Supplementary Data Table S3), and QTLs associated with most of these traits for these two mineral elements were co-located (Supplementary Data Table S6). Co-localization of QTLs associated with ionomic traits of different mineral elements were reported for shoot Ca/Mg in *B. oleracea* (Broadley *et al.*, 2008), shoot Mg/Sr in *B. rapa* (Wu et *al.*, 2008), rosette K/Mg/Zn in Arabidopsis (Ghandilyan *et al.*, 2009*a*), shoot B/Cu, B/P and Ca/Mg (Liu *et al.*, 2009), seed Ca/Mg and

Cu/Fe/Mn/Zn (Ding *et al.*, 2010), and shoot Cu/Mn/Zn (Bus *et al.*, 2014) in *B. napus*. Together, these findings reflect the observation that some mineral elements share common uptake and transport pathways (White *et al.*, 2012*a, b*), especially those mineral elements with chemical similarities, such as Ca and Mg, or Ca and Mn observed in this study. Mei *et al.* (2007) found that expression of an activated Arabidopsis Ca^{2+}/H^{+} antiporter CAX1 variant that increased Ca accumulation also increased concentrations of other mineral elements, such as Mg and Mn, in the root of tobacco.

It is anticipated that studies of the genetic basis of shoot mineral element composition will contribute to improvements in the nutritional content of leafy vegetables, such as *B. rapa* and *B. oleracea* (White and Broadley, 2009). In this study, ten QTL clusters were identified that affected shoot concentrations and/or contents of more than two mineral elements but did not affect SDW (Fig. 6; Supplementary Data Table S6). Among these QTL clusters, the QTL cluster Cl17.1 on chromosome C07 had a significant effect on both shoot Mg and S concentrations at LP (Fig. 7). Glucosinolates are a group of sulfur-rich secondary metabolites that are abundant in Brassicaceae. An obvious phenotypic segregation is observed for total glucosinolate concentration and the majority of the individual glucosinolates in seeds and leaves in the *Bna*TNDH population (Feng *et al.*, 2012). Sulfur concentration is tightly positive correlated with glucosinolate concentrations in seed (Körber *et al.*, 2016) and the QTL cluster Cl17.1 was co-located with QTLs affecting seed concentrations of three different glucosinolates (4-methylsulfinylbutyl glucosinolate, 2-hydroxy-4-pentenyl glucosinolate and 3-indolyl-methyl glucosinolate) previously identified in the

*Bna*TNDH population (Feng *et al.*, 2012). This major QTL cluster was further narrowed down to a 28.5–30.6 Mb region in which 236 annotated genes were located (Supplementary Data Table S9). There was a promising candidate gene, *BnaC07g22430D* (homologous to *At2G03620*, magnesium transporter 3), for Mg transport in this region but no obvious candidate genes for S transport. Further research should be conducted to investigate if the pleiotropic effect of this locus is conferred by one gene or two closely linked genes.

Epistatic interactions for the ionomic traits

A total of 54 epistatic interactions were identified for various ionomic traits in the *Bna*TNDH population at OP and LP (Table 4), but most of these epistatic interactions did not involve any additive QTL (Supplementary Data Table S5). A number of epistatic interactions were also found for different ionomic traits in Arabidopsis (Ghandilyan *et al.*, 2009*b*) and *B. napus* (Liu *et al.*, 2009). The large number of epistatic interactions discovered in this study suggest a complex genetic network controlling the *B. napus* ionome at both OP and LP. The epistatic interactions could account for 0–48.7% of the phenotypic variation for different ionomic traits, implying that epistasis is a major genetic component for some ionomic traits. The additive QTLs could explain between 0–51.9% of the phenotypic variation for different ionomic traits, suggesting that it might be feasible to improve ionomic traits genetically.

CONCLUSIONS

The reductions in plant Ca, Cu, K, Mg, Mn, Na and Zn contents in P-deficient *B. napus* are likely to be a consequence of reduced growth. The Fe concentration was higher in plants at LP than at OP, possibly because P and Fe can precipitate together when Pi concentrations are high, which results in reduced Fe availability. Significant positive correlations were observed among many ionomic traits across P treatments, which could be the result of element-element interactions, but also could result from the genetic linkage of QTLs controlling traits for different elements. Six QTL clusters were associated with more than three traits impacting mineral element composition, suggesting that some mineral elements share common uptake and transport pathways. Near-isogenic lines should be developed to allow finer mapping of the quantitative genes underpinning the major QTLs identified in this study. This will contribute to a greater understanding of processes affecting the uptake and partitioning of mineral elements in *B. napus*.

SUPPLEMENTARY DATA

Figure S1: frequency distribution of shoot concentrations of eleven mineral elements in the *Bna*TNDH mapping population grown at an optimal (OP) and a low P supply (LP). Figure S2: frequency distribution of root concentrations of eleven mineral elements in the *Bna*TNDH mapping population grown at an optimal (OP) and a low P supply (LP). Figure S3: frequency distribution of shoot contents of eleven mineral elements in the *Bna*TNDH mapping population grown at an optimal (OP) and a low P supply (LP). Figure S4: frequency distribution of root contents of eleven mineral elements in the *Bna*TNDH mapping population grown at an optimal (OP) and a low P supply (LP). Figure S5: frequency distribution of plant contents of eleven mineral elements in the *Bna*TNDH mapping population grown at an optimal (OP) and a low P supply (LP). Figure S6: frequency distribution of partitioning to the shoot of eleven mineral elements in the *Bna*TNDH mapping population grown at an optimal (OP) and a low P supply (LP). Table S1: shoot and root concentrations of eleven mineral elements in the *Bna*TNDH lines and their parents at an optimal (OP) and a low P supply (LP). Table S2: shoot and root contents (μg plant^{-1}) of eleven mineral elements in the *Bna*TNDH lines and their parents at an optimal (OP) and a low P supply (LP). Table S3: Pearson's correlation coefficients among shoot contents and among root contents of eleven mineral elements in the *Bna*TNDH mapping population at an optimal (upper right triangle) and a low P supply (lower left triangle). Table S4: plant contents (μg plant^{-1}) and partitioning to the shoot (%) of eleven mineral elements in the *Bna*TNDH lines and their parents at an optimal (OP) and a low P supply (LP). Table S5: the number and

explained phenotypic variation of the additive QTL and epistatic QTL for shoot and root concentrations, shoot, root and plant contents, and partitioning to the shoot of eleven mineral elements detected in the *Bna*TNDH population at an optimal (OP) and a low P supply (LP). Table S6: meta-analysis of QTL clusters for shoot and root concentrations, shoot, root and plant contents, and partitioning to the shoot of eleven mineral elements, shoot dry weight, root dry weight and total dry weight in the *Bna*TNDH population at an optimal and a low P supply. Table S7: Pearson's correlation coefficients between root traits and shoot concentrations of eleven mineral elements in the *Bna*TNDH mapping population at an optimal (OP) and a low P supply (LP). Table S8: Pearson's correlation coefficients between shoot and root concentrations of eleven mineral elements in the *Bna*TNDH mapping population at an optimal (OP) and a low P supply (LP). Table S9: annotated genes underlying the QTL cluster Cl17.1 in *Brassica napus*.

ACKNOWLEDGEMENTS

This research was supported by the Applied Basic Research Fronts Program of Wuhan city (2018020401011302), the National Key R&D Program of China (Grant No. 2017YFD0200200), National Nature Science Foundation of China (Grant No. 31972498), Natural and Fundamental Research Funds for the Central Universities of China (Grant No. 2662019PY013) and the Rural and Environment Science and Analytical Services Division (RESAS) of the Scottish Government.

LITERATURE CITED

Alcock TD, Havlickova L, He Z, *et al.* 2017. Identification of candidate genes for calcium and magnesium accumulation in *Brassica napus* L. by association genetics. *Frontiers in Plant Science* **8:** 1968.

Alcock TD, Havlickova L, He Z, *et al.* 2018. Species-wide variation in shoot nitrate concentration, and genetic loci controlling nitrate, phosphorus and potassium accumulation in *Brassica napus* L. *Frontiers in Plant Science* **9:** 1487.

Andrés-Colás N, Sancenón V, Rodríguez-Navarro S, *et al.* 2006. The Arabidopsis heavy metal P-type ATPase HMA5 interacts with metallochaperones and functions in copper detoxification of roots. *The Plant Journal* **45:** 225–236.

Arcade A, Labourdette A, Falque M, *et al.* 2004. BioMercator: integrating genetic maps and QTL towards discovery of candidate genes. *Bioinformatics* **20:** 2324–2326.

Atwell S, Huang YS, Vilhjálmsson BJ, *et al.* 2010. Genome-wide association study of 107 phenotypes in *Arabidopsis thaliana* inbred lines. *Nature* **465:** 627–631.

Balzergue C, Dartevelle T, Godon C, *et al.* 2017. Low phosphate activates STOP1-ALMT1 to rapidly inhibit root cell elongation. *Nature Communications* **8:** 15300.

Baxter I. 2009. Ionomics: studying the social network of mineral nutrients. *Current Opinion in Plant Biology* **12:** 381–386.

Baxter IR, Vitek O, Lahner B, *et al.* 2008. The leaf ionome as a multivariable system to detect a plant's physiological status. *Proceedings of the National Academy of Sciences, USA* **105:** 12081–12086.

Bentsink L, Yuan K, Koornneef M, Vreugdenhil D. 2003. The genetics of phytate and phosphate accumulation in seeds and leaves of *Arabidopsis thaliana*, using natural variation. *Theoretical and Applied Genetics* **106:** 1234–1243.

Black JR, Yin Q, Casey WH. 2006. An experimental study of magnesium-isotope fractionation in chlorophyll-a photosynthesis. *Geochimica et Cosmochimica Acta* **70:** 4072–4079.

Broadley MR, Hammond JP, King GJ, *et al.* 2008. Shoot calcium and magnesium concentrations differ between subtaxa, are highly heritable, and associate with potentially pleiotropic loci in *Brassica oleracea*. *Plant Physiology* **146:** 1707–1720.

Bus A, Körber N, Parkin IA, *et al.* 2014. Species- and genome-wide dissection of the shoot ionome in *Brassica napus* and its relationship to seedling development. *Frontiers in Plant Science* **5:** 485.

Chalhoub B, Denoeud F, Liu S, *et al.* 2014. Early allopolyploid evolution in the post-Neolithic *Brassica napus* oilseed genome. *Science* **345:** 950–953.

Coque M, Martin A, Veyrieras JB, Hirel B, Gallais A. 2008. Genetic variation for N-remobilization and postsilking N-uptake in a set of maize recombinant inbred lines. 3. QTL detection and coincidences. *Theoretical and Applied Genetics* **117:** 729–747.

Dalton CC, Iqbal K, Turner DA. 1983. Iron phosphate precipitation in Murashige and Skoog media. *Physiologia Plantarum* **57:** 472–476.

Ding G, Yang M, Hu Y, *et al.* 2010. Quantitative trait loci affecting seed mineral

concentrations in *Brassica napus* grown with contrasting phosphorus supplies. *Annals of Botany* **105:** 1221–1234.

Duan HY, Shi L, Ye XS, Wang YH, Xu FS. 2009. Identification of phosphorous efficient germplasm in oilseed rape. *Journal of Plant Nutrition* **32:** 1148–1163.

Durrett TP, Gassmann W, Rogers EE. 2007. The FRD3-mediated efflux of citrate into the root vasculature is necessary for efficient iron translocation. *Plant Physiology* **144:** 197–205.

Feng J, Long Y, Shi L, Shi J, Barker G, Meng J. 2012. Characterization of metabolite quantitative trait loci and metabolic networks that control glucosinolate concentration in the seeds and leaves of *Brassica napus*. *New Phytologist* **193:** 96–108.

Ghandilyan A, Barboza L, Tisné S, *et al.* 2009*a*. Genetic analysis identifies quantitative trait loci controlling rosette mineral concentrations in *Arabidopsis thaliana* under drought. *New Phytologist* **184:** 180–192.

Ghandilyan A, Ilk N, Hanhart C, *et al.* 2009*b*. A strong effect of growth medium and organ type on the identification of QTLs for phytate and mineral concentrations in three *Arabidopsis thaliana* RIL populations. *Journal of Experimental Botany* **60:** 1409–1425.

Goffinet B, Gerber S. 2000. Quantitative trait loci: a meta-analysis. *Genetics* **155:** 463–473.

Gruber BD, Giehl RF, Friedel S, von Wirén N. 2013. Plasticity of the Arabidopsis root system under nutrient deficiencies. *Plant Physiology* **163:** 161–179.

Grusak MA, Broadley MR, White PJ. 2016. Plant macro- and micronutrient minerals (Version 2.0). In: eLS, John Wiley & Sons, Chichester UK. doi: 10.1002/9780470015902.a0001306.pub2

Gutiérrez-Alanís D, Ojeda-Rivera JO, Yong-Villalobos L, Cárdenas-Torres L, Herrera-Estrella L. 2018. Adaptation to phosphate scarcity: tips from *Arabidopsis* roots. *Trends in Plant Science* **23:** 721–730.

Hammond JP, Broadley MR, White PJ, *et al.* 2009. Shoot yield drives phosphorus use efficiency in *Brassica oleracea* and correlates with root architecture traits. *Journal of Experimental Botany* **60:** 1953–1968.

Harada H, Leigh RA. 2006. Genetic mapping of natural variation in potassium concentrations in shoots of *Arabidopsis thaliana*. *Journal of Experimental Botany* **57:** 953–960.

Hawkesford M, Horst W, Kichey T, *et al.* 2012. Functions of macronutrients. In: Marschner P, ed. *Marschner's Mineral Nutrition of Higher Plants*. London: Academic Press, 135–189.

Huang XY, Salt DE. 2016. Plant ionomics: from elemental profiling to environmental adaptation. *Molecular Plant* **9:** 787–797.

Kering MK, Lukaszewska K, Blevins DG. 2009. Manganese requirement for optimum photosynthesis and growth in NAD-malic enzyme C-4 species. *Plant and Soil* **316:** 217–226.

Kobayashi Y, Kuroda K, Kimura K, *et al.* 2008. Amino acid polymorphisms in strictly conserved domains of a P-type ATPase HMA5 are involved in the

mechanism of copper tolerance variation in Arabidopsis. *Plant Physiology* **148:** 969–980.

Koprivova A, Harper AL, Trick M, Bancroft I, Kopriva S. 2014. Dissection of the control of anion homeostasis by associative transcriptomics in *Brassica napus*. *Plant Physiology* **166:** 442–450.

Körber N, Bus A, Li J, *et al.* 2016. Agronomic and seed quality traits dissected by genome-wide association mapping in *Brassica napus*. *Frontiers in Plant Science* **7:** 386.

Lahner B, Gong J, Mahmoudian M, *et al.* 2003. Genomic scale profiling of nutrient and trace elements in *Arabidopsis thaliana*. *Nature Biotechnology* **21:** 1215–1221.

Li Y, Wang X, Zhang H, *et al.* 2019. Molecular identification of the phosphate tr ansporter family 1 (PHT1) genes and their expression profiles in response to ph osphorus deprivation and other abiotic stresses in *Brassica napus*. *PLoS One* **1 4:** e0220374.

Liu J, Yang J, Li R, *et al.* 2009. Analysis of genetic factors that control shoot mineral concentrations in rapeseed (*Brassica napus*) in different boron environments. *Plant and Soil* **320:** 255–266.

Loudet O, Chaillou S, Merigout P, Talbotec J, Daniel-Vedele F. 2003. Quantitative trait loci analysis of nitrogen use efficiency in Arabidopsis. *Plant Physiology* **131:** 345–358.

Loudet O, Saliba-Colombani V, Camilleri C, *et al.* 2007. Natural variation for sulfate content in *Arabidopsis thaliana* is highly controlled by APR2. *Nature Genetics* **39:**

896–900.

Maillard A, Etienne P, Diquélou S, *et al.* 2016. Nutrient deficiencies modify the ionomic composition of plant tissues: a focus on cross-talk between molybdenum and other nutrients in *Brassica napus*. *Journal of Experimental Botany* **67:** 5631–5641.

Mäser P, Thomine S, Schroeder JI, *et al.* 2001. Phylogenetic relationships within cation transporter families of Arabidopsis. *Plant Physiology* **126:** 1646–1667.

Mei H, Zhao J, Pittman JK, Lachmansingh J, Park S, Hirschi KD. 2007. *In planta* regulation of the *Arabidopsis* Ca^{2+}/H^{+} antiporter CAX1. *Journal of Experimental Botany* **58:** 3419–3427.

Meng L, Li H, Zhang L, Wang J. 2015. QTL IciMapping: integrated software for genetic linkage map construction and quantitative trait locus mapping in bi-parental populations. *The Crop Journal* **3:** 265–279.

Müller J, Toev T, Heisters M, *et al.* 2015. Iron-dependent callose deposition adjusts root meristem maintenance to phosphate availability. *Developmental Cell* **33:** 216–230.

Murashige T, Skoog F. 1962. A revised medium for rapid growth and bioassays with tobacco tissue cultures. *Physiologia Plantarum* **15:** 473–497.

Neugebauer K, Broadley MR, El-Serehy HA, *et al.* 2018. Variation in the angiosperm ionome. *Physiologia Plantarum* **163:** 306–322.

Neugebauer K, El-Serehy HA, George TS, *et al.* 2019. The influence of phylogeny and ecology on root, shoot and plant ionomes of fourteen native Brazilian species.

Physiologia Plantarum, in press. doi: 10.1111/ppl.13018.

Paran I, Zamir D. 2003. Quantitative traits in plants: beyond the QTL. *Trends in Genetics* **19:** 303–306.

Payne KA, Bowen HC, Hammond JP, *et al.* 2004. Natural genetic variation in caesium (Cs) accumulation by *Arabidopsis thaliana*. *New Phytologist* **162:** 535–548.

Pongrac P, Fischer S, Thompson JA, Wright G, White PJ. 2020. Early responses of *Brassica oleracea* roots to zinc supply under sufficient and sub-optimal phosphorus supply. *Frontiers in Plant Science* **10:** 1645.

Puig S, Andrés-Colás N, García-Molina A, Peñarrubia L. 2007. Copper and iron homeostasis in *Arabidopsis*: responses to metal deficiencies, interactions and biotechnological applications. *Plant, Cell & Environment* **30:** 271–290.

Qiu D, Morgan C, Shi J, *et al.* 2006. A comparative linkage map of oilseed rape and its use for QTL analysis of seed oil and erucic acid content. *Theoretical and Applied Genetics* **114:** 67–80.

Salt DE, Baxter I, Lahner B. 2008. Ionomics and the study of the plant ionome. *Annual Review of Plant Biology* **59:** 709–733.

Sánchez-Bermejo E, Castrillo G, del Llano B, *et al.* 2014. Natural variation in arsenate tolerance identifies an arsenate reductase in *Arabidopsis thaliana*. *Nature Communications* **5:** 4617.

Sharpe AG, Lydiate DJ. 2003. Mapping the mosaic of ancestral genotypes in a cultivar of oilseed rape (*Brassica napus*) selected via pedigree breeding. *Genome* **46:** 461–

468.

Shi L, Shi T, Broadley MR, *et al.* 2013. High-throughput root phenotyping screens identify genetic loci associated with root architectural traits in *Brassica napus* under contrasting phosphate availabilities. *Annals of Botany* **112:** 381–389.

Thomas CL, Alcock TD, Graham NS, *et al.* 2016*a*. Root morphology and seed and leaf ionomic traits in a *Brassica napus* L. diversity panel show wide phenotypic variation and are characteristic of crop habit. *BMC Plant Biology* **16:** 214.

Thomas CL, Graham NS, Hayden R, *et al.* 2016*b*. High-throughput phenotyping (HTP) identifies seedling root traits linked to variation in seed yield and nutrient capture in field-grown oilseed rape (*Brassica napus* L.). *Annals of Botany* **118:** 655–665.

von Wirén N, Klair S, Bansal S, *et al.* 1999. Nicotianamine chelates both Fe^{III} and Fe^{II}. Implications for metal transport in plants. *Plant Physiology* **119:** 1107–1114.

Vreugdenhil D, Aarts MGM, Koornneef M, Nelissen H, Ernst WHO. 2004. Natural variation and QTL analysis for cationic mineral content in seeds of *Arabidopsis thaliana*. *Plant, Cell & Environment* **27:** 828–839.

Wang W, Ding GD, White PJ, *et al.* 2019. Mapping and cloning of quantitative trait loci for phosphorus efficiency in crops: opportunities and challenges. *Plant and Soil* **439:** 91–112.

Ward JT, Lahner B, Yakubova E, Salt DE, Raghothama KG. 2008. The effect of iron on the primary root elongation of Arabidopsis during phosphate deficiency. *Plant Physiology* **147:** 1181–1191.

Watanabe T, Urayama M, Shinano T, Okada R, Osaki M. 2015. Application of ionomics to plant and soil in fields under long-term fertilizer trials. *SpringerPlus* **4:** 781.

Waters BM, Grusak MA. 2008. Quantitative trait locus mapping for seed mineral concentrations in two *Arabidopsis thaliana* recombinant inbred populations. *New Phytologist* **179:** 1033–1047.

Welch RM. 1995. Micronutrient nutrition of plants. *Critical Reviews in Plant Sciences* **14:** 49–82.

White PJ, Broadley MR. 2009. Biofortification of crops with seven mineral elements often lacking in human diets – iron, zinc, copper, calcium, magnesium, selenium and iodine. *New Phytologist* **182:** 49–84.

White PJ, George TS, Gregory PJ, Bengough AG, Hallett PD, McKenzie BM. 2013. Matching roots to their environment. *Annals of Botany* **112:** 207–222.

White PJ, Hammond JP, King GJ, *et al.* 2010. Genetic analysis of potassium use efficiency in *Brassica oleracea*. *Annals of Botany* **105:** 1199–1210.

White PJ. 2012*a*. Ion uptake mechanisms of individual cells and roots: short-distance transport. In: Marschner P, ed. *Marschner's Mineral Nutrition of Higher Plants*. London: Academic Press, 7–47.

White PJ. 2012*b*. Long-distance transport in the xylem and phloem. In: Marschner P, ed. *Marschner's Mineral Nutrition of Higher Plants*. London: Academic Press, 49–70.

Wu D, Sato K, Ma JF. 2015. Genome-wide association mapping of cadmium

accumulation in different organs of barley. *New Phytologist* **208:** 817-829.

Wu J, Yuan YX, Zhang XW, *et al.* 2008. Mapping QTLs for mineral accumulation and shoot dry biomass under different Zn nutritional conditions in Chinese cabbage (*Brassica rapa* L. ssp. *pekinensis*). *Plant and Soil* **310:** 25–40.

Xiao Y, Liu H, Wu L, Warburton M, Yan J. 2017. Genome-wide association studies in maize: praise and stargaze. *Molecular Plant* **10:** 359–374.

Yang M, Lu K, Zhao FJ *et al.* 2018. Genome-wide association studies reveal the genetic basis of ionomic variation in rice. *The Plant Cell* **30:** 2720–2740.

Zeng LP. 2011. *Construction of reciprocal introgression lines and evaluation in* Brassica napus *L*. Master Thesis, Huazhong Agricultural University, China.

Zhang Y, Thomas CL, Xiang J, *et al.* 2016. QTL meta-analysis of root traits in *Brassica napus* under contrasting phosphorus supply in two growth systems. *Scientific Reports* **6:** 33113.

Zhao J, Jamar DC, Lou P, *et al.* 2008. Quantitative trait loci analysis of phytate and phosphate concentrations in seeds and leaves of *Brassica rapa*. *Plant, Cell & Environment* **31:** 887–900.

Figure legends

Fig. 1. Shoot (A) and root concentrations (B) of eleven mineral elements in cultivars Tapidor and Ningyou 7 grown in various environments. Shoot concentrations of B, Ca, Cu, Fe, Mg, P and Zn were determined in three studies (study 1, 2 and 3), comprising eleven growth environments: two environments were from study 1 (0.25 and 50 μM B in a hydroponic system, Liu *et al.*, 2009), five from study 2-1 (0, 6, 312.5, 625 and 1250 μM P in an agar system, Shi *et al.*, 2013), two from study 2-2 (0 and 625 μM P in an agar system, Shi *et al.*, 2013), and two from study 3 (0 and 625 μM P in an agar system in the present paper); Shoot concentrations of K and Mn were from nine environments, of which five were from study 2-1, two were from study 2-2, and two were from study 3; Shoot concentrations of Na and S were from seven environments, of which five were from study 2-1 and two were from study 2-2; Root concentrations of B, Ca, Cu, Fe, K, Mg, Mn, P and Zn were from nine environments, of which five were from study 2-1, two were from study 2-2, and two were from study 3; Root concentrations of Na and S were from seven environments, of which five were from study 2-1 and two were from study 2-2. The two walls of the box correspond to first and third quartiles. Whiskers are separated from the box by a 1.5 interquartile range (3rd quartile minus 1st quartile). Circles represent individual measures outside the whiskers. The central black line in the box is a median. A significant difference for each mineral element tested by one-sample *t* test between the mean and 1 is indicated by an asterisk (*$P < 0.05$, **$P < 0.01$).

Figure 1.

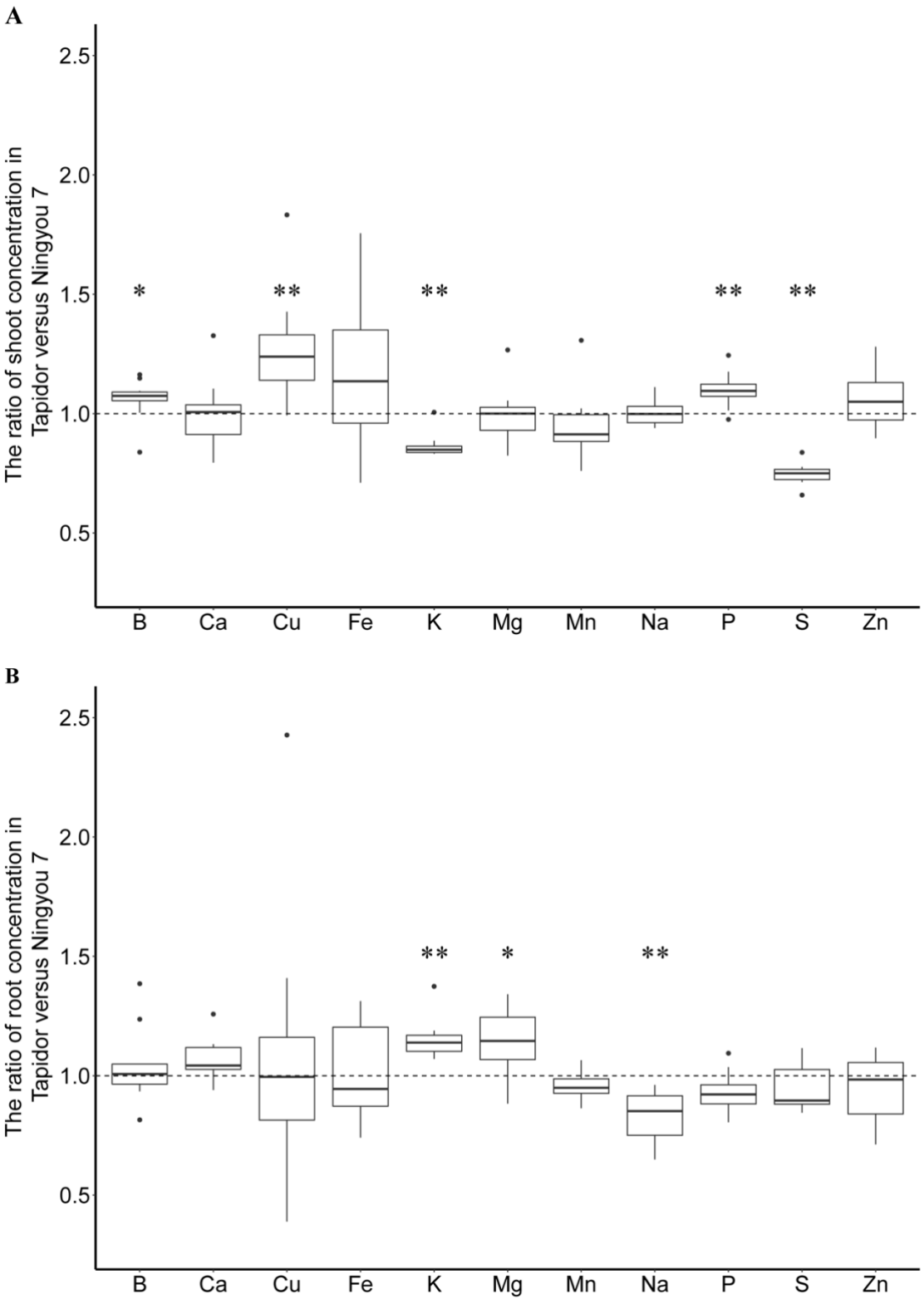
A
The ratio of shoot concentration in Tapidor versus Ningyou 7
2.5
2.0
1.5
1.0
0.5
*
**
**
**
**
B
Ca
Cu
Fe
K
Mg
Mn
Na
P
S
Zn
B
The ratio of root concentration in Tapidor versus Ningyou 7
2.5
2.0
1.5
1.0
0.5
**
*
**
B
Ca
Cu
Fe
K
Mg
Mn
Na
P
S
Zn

Fig. 2. The effect of P deficiency on shoot (A) and root concentrations (B) of eleven mineral elements in Tapidor and Ningyou 7. The data for Tapidor and Ningyou 7 at a low P supply (LP) were scaled to that of cultivars Tapidor and Ningyou 7 at an optimal P supply (OP). The black dotted line indicates shoot and root concentrations of the eleven mineral elements of Tapidor and Ningyou 7 at OP (Supplementary Data Table S1). The black and gray lines indicate shoot and root concentrations of the eleven mineral elements in Tapidor and Ningyou 7 at LP, respectively. Traits that show a significant difference between the two P treatments are labelled by a black asterisk for Tapidor and a gray asterisk for Ningyou 7 (*P < 0.05, Student's t-test). Each trait contains eight to eleven biological replicates.

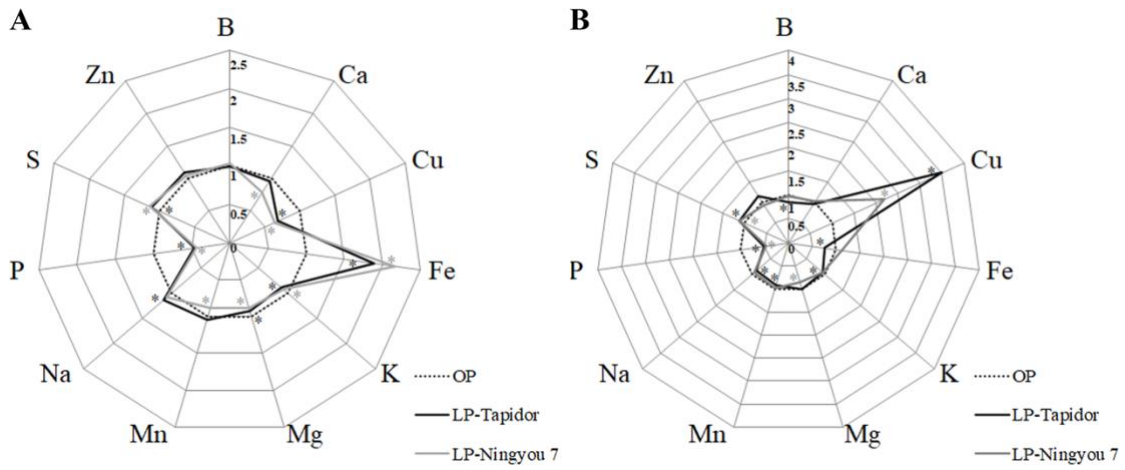

Fig. 3. Shoot and root concentrations, shoot, root and plant contents, and partitioning to the shoot of eleven mineral elements in the *Bna*TNDH population grown at an optimal (OP) and a low P supply (LP). Boxes represent the mid two quartiles with the median drawn; whiskers are the 95% confidence limits, and extreme values are plotted individually. For each trait, a significant difference between two P treatments is labelled by an asterisk (*$P < 0.05$, **$P<0.01$, Student's *t*-test).

Figure 3

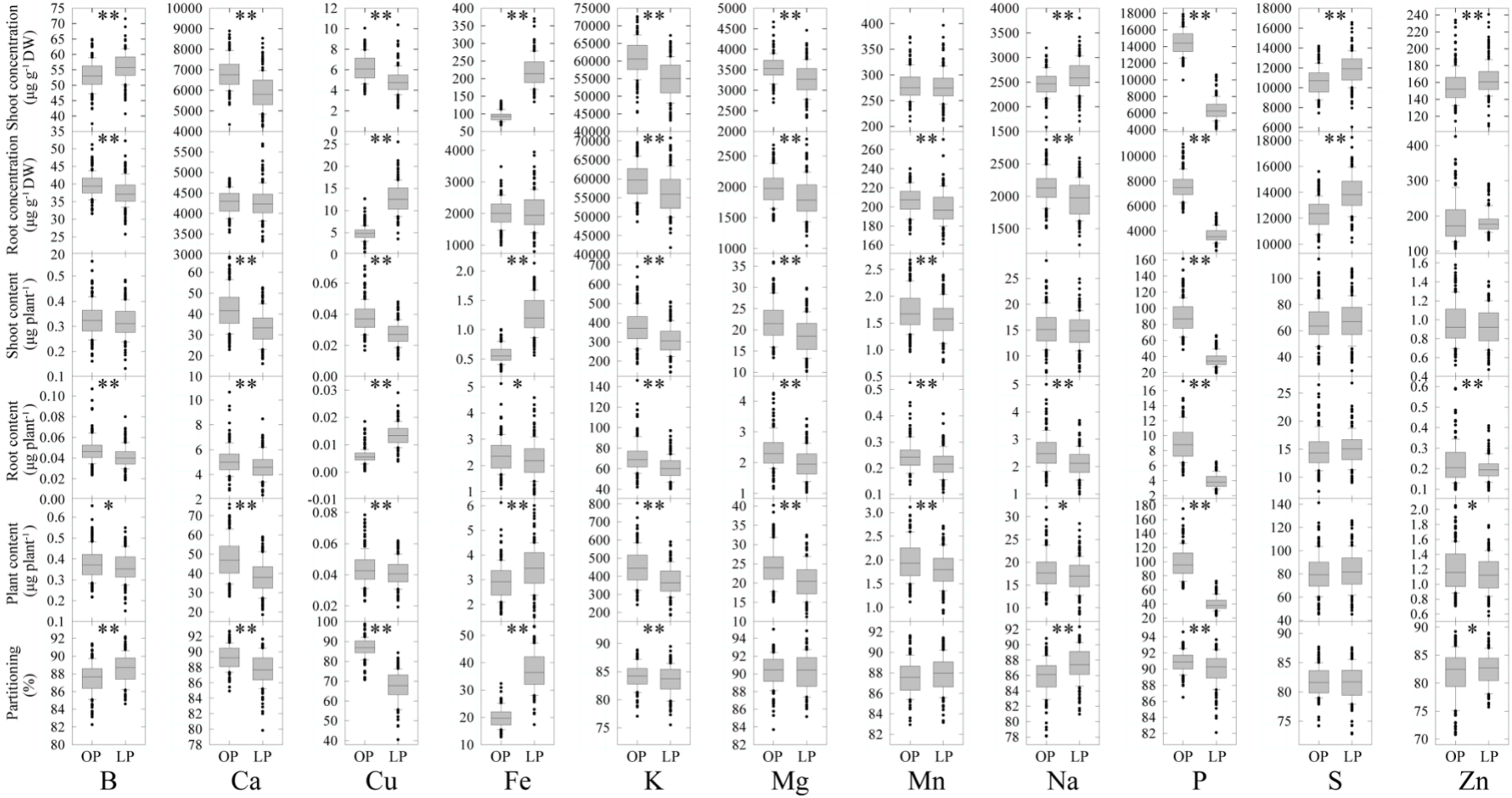
Shoot concentration (µg g-1 DW)
Root concentration (µg g-1 DW)
Shoot content (µg plant-1)
Root content (µg plant-1)
Plant content (µg plant-1)
Partitioning (%)
OP
LP
B
Ca
Cu
Fe
K
Mg
Mn
Na
P
S
Zn

Fig. 4. Principal component (PC) plot of the first two PC scores of shoot and root concentrations of eleven mineral elements in the *Bna*TNDH population at an optimal (A) and a low P supply (B). Colours indicate organs (black = shoot, gray = root).

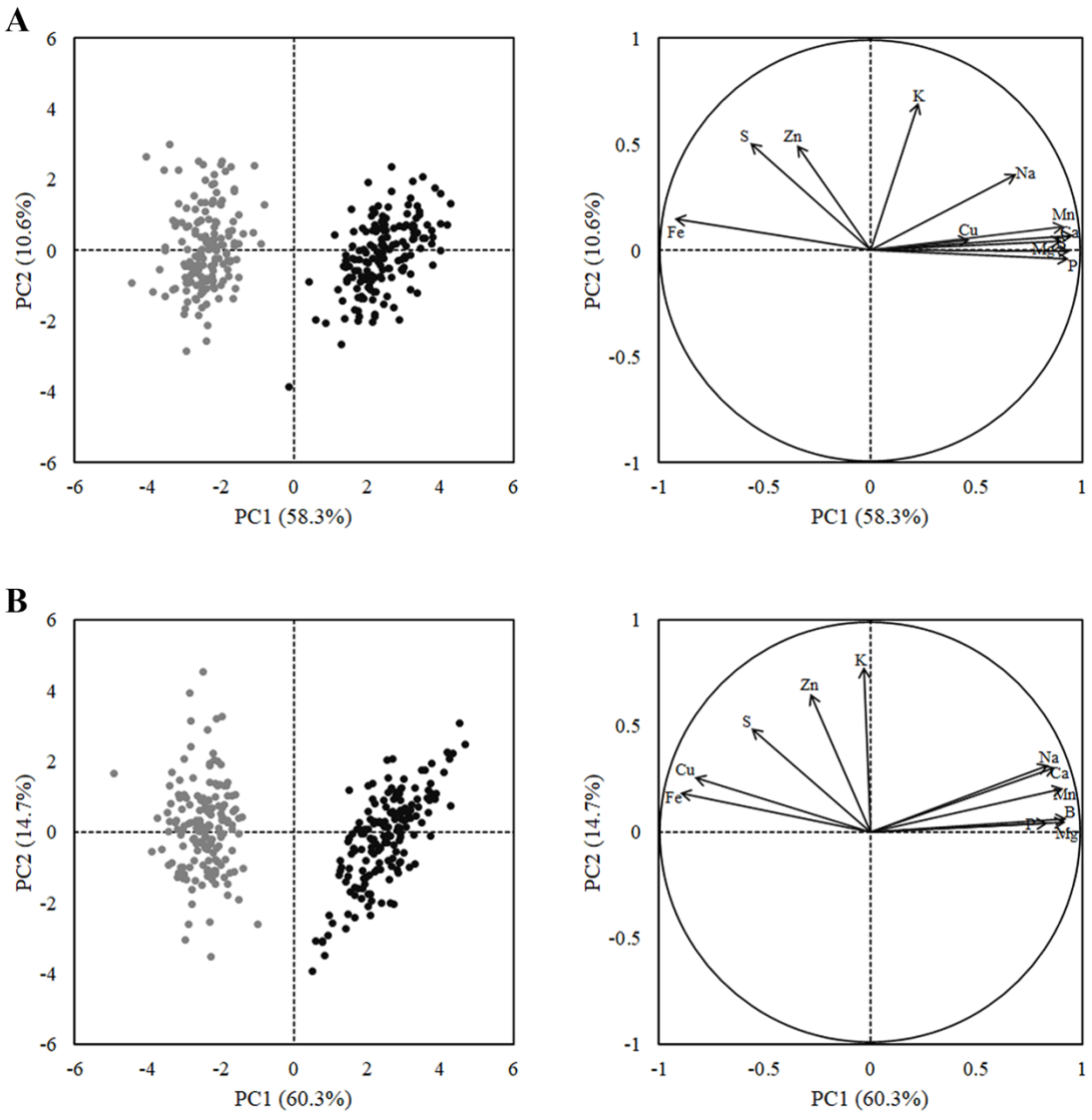

Fig. 5. The epistatic QTLs for shoot and root concentrations, shoot, root and plant contents, and partitioning to the shoot of eleven mineral elements as well as the total dry weight (TDW) at an optimal (A) and a low P supply (B). The circle indicates the 19 linkage groups and the black and gray lines denote the epistatic interactions between each two loci for different traits. Two pleiotropic epistatic QTLs are presented at both optimal and low P supplies. Each ionomic trait was denominated as "S (abbreviation of shoot) or R (abbreviation of root) or P (abbreviation of plant) + [mineral element] + conc (abbreviation of concentration) or cont (abbreviation of content) or part (abbreviation of partitioning)".

Figure 5

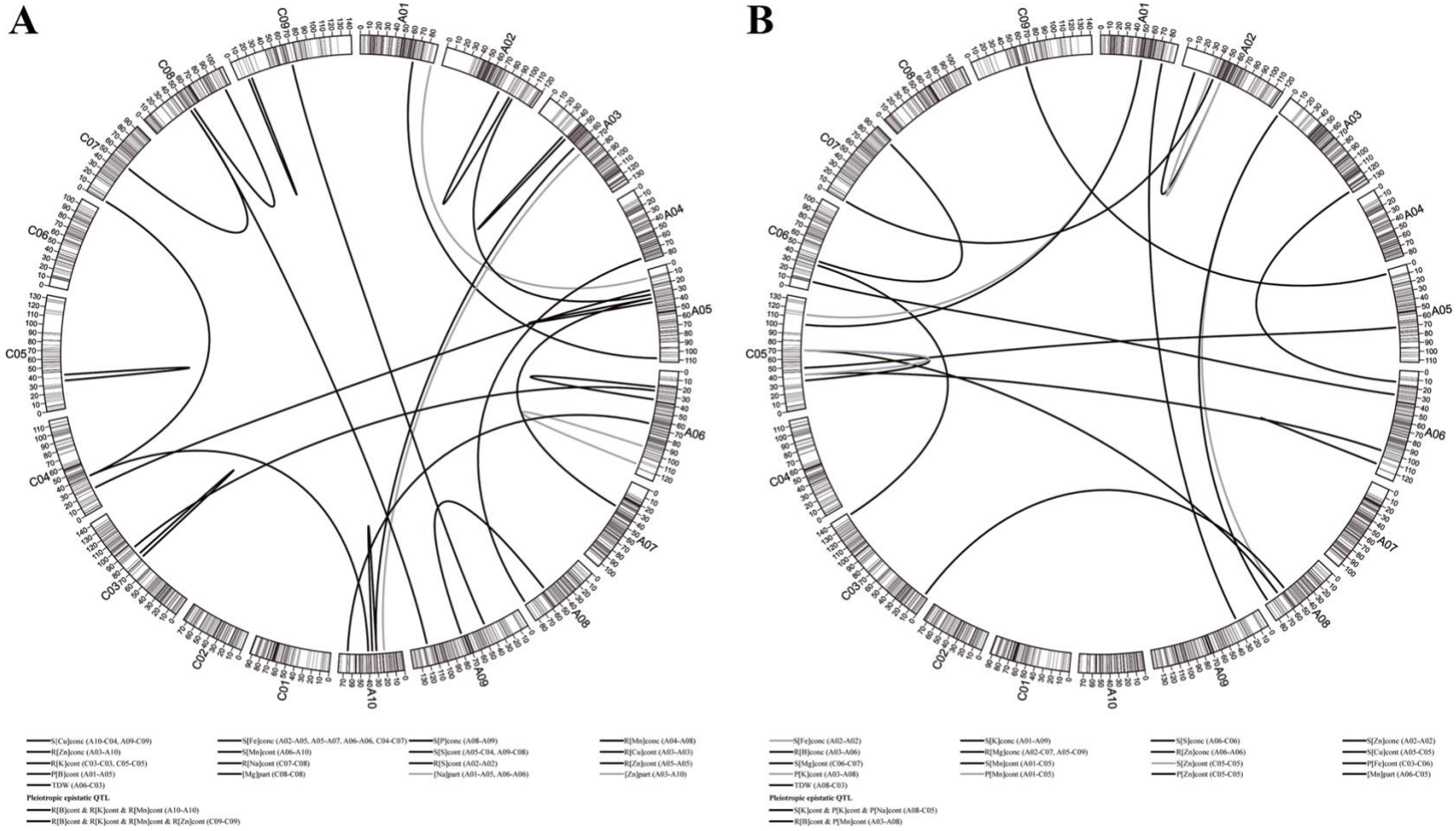
A
B
S[Cu]conc (A10-C04, A09-C09)
R[Zn]conc (A03-A10)
R[K]cont (C03-C03, C05-C05)
P[B]cont (A01-A05)
TDW (A06-C03)
Pleiotropic epistatic QTL
R[B]cont & R[K]cont & R[Mn]cont (A10-A10)
R[B]cont & R[K]cont & R[Mn]cont & R[Zn]cont (C09-C09)
S[Fe]conc (A02-A05, A05-A07, A06-A06, C04-C07)
S[Mn]cont (A06-A10)
R[Na]cont (C07-C08)
[Mg]part (C08-C08)
S[P]conc (A08-A09)
S[S]cont (A05-C04, A09-C08)
R[S]cont (A02-A02)
[Na]part (A01-A05, A06-A06)
R[Mn]conc (A04-A08)
R[Cu]conc (A03-A03)
R[Zn]conc (A05-A05)
[Zn]part (A03-A10)
S[Fe]conc (A02-A02)
R[B]conc (A03-A06)
S[Mg]conc (C06-C07)
P[K]cont (A03-A08)
TDW (A08-C03)
Pleiotropic epistatic QTL
S[K]cont & P[K]cont & P[Na]cont (A08-C05)
R[B]cont & P[Mn]cont (A03-A08)
S[K]conc (A01-A09)
R[Mg]conc (A02-C07, A05-C09)
S[Mn]cont (A01-C05)
P[Mn]cont (A01-C05)
S[S]conc (A06-C06)
R[Zn]conc (A06-A06)
S[Zn]cont (C05-C05)
P[Zn]cont (C05-C05)
S[Zn]conc (A02-A02)
S[Cu]cont (A03-C05)
P[Fe]cont (C03-C06)
[Mn]part (A06-C05)

Fig. 6. Location of the QTL clusters for shoot and root concentrations, shoot, root and plant contents, and partitioning to the shoot of eleven mineral elements in the *Bna*TNDH population grown at an optimal (OP) and a low P supply (LP) identified by meta-QTL analysis. The vertical columns represented linkage groups of the *Bna*TNDH population. The black blocks inside each vertical column represent the QTL clusters. The name of each QTL cluster is on the right of the linkage group. The number in brackets indicates the number of mineral elements controlled by different QTL clusters.

Figure 6

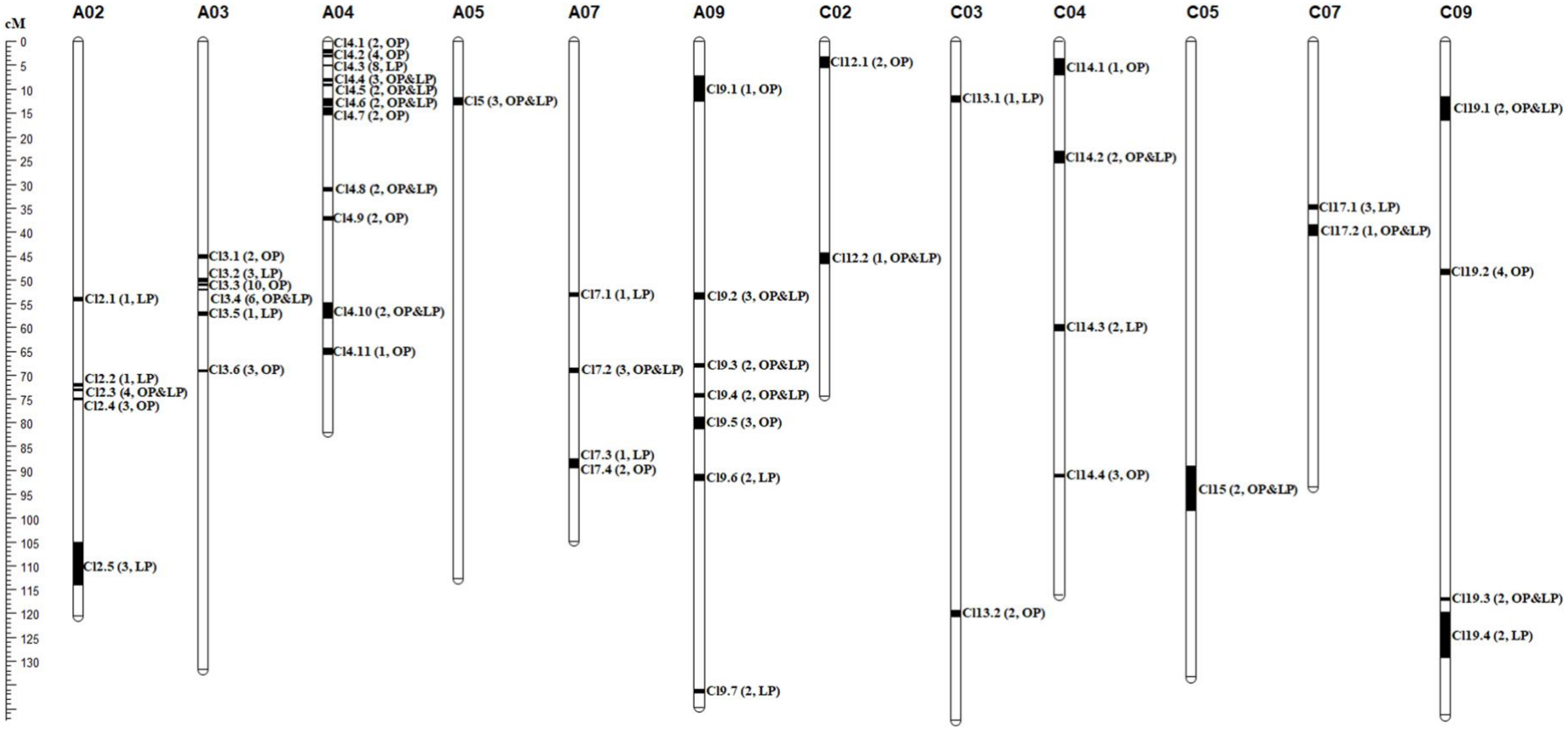
cM
A02
A03
A04
A05
A07
A09
C02
C03
C04
C05
C07
C09
C12.1 (1, LP)
C12.2 (1, LP)
C12.3 (4, OP&LP)
C12.4 (3, OP)
C12.5 (3, LP)
C13.1 (2, OP)
C13.2 (3, LP)
C13.3 (10, OP)
C13.4 (6, OP&LP)
C13.5 (1, LP)
C13.6 (3, OP)
C14.1 (2, OP)
C14.2 (4, OP)
C14.3 (8, LP)
C14.4 (3, OP&LP)
C14.5 (2, OP&LP)
C14.6 (2, OP&LP)
C14.7 (2, OP)
C14.8 (2, OP&LP)
C14.9 (2, OP)
C14.10 (2, OP&LP)
C14.11 (1, OP)
C15 (3, OP&LP)
C17.1 (1, LP)
C17.2 (3, OP&LP)
C17.3 (1, LP)
C17.4 (2, OP)
C19.1 (1, OP)
C19.2 (3, OP&LP)
C19.3 (2, OP&LP)
C19.4 (2, OP&LP)
C19.5 (3, OP)
C19.6 (2, LP)
C19.7 (2, LP)
C112.1 (2, OP)
C112.2 (1, OP&LP)
C113.1 (1, LP)
C113.2 (2, OP)
C114.1 (1, OP)
C114.2 (2, OP&LP)
C114.3 (2, LP)
C114.4 (3, OP)
C115 (2, OP&LP)
C117.1 (3, LP)
C117.2 (1, OP&LP)
C119.1 (2, OP&LP)
C119.2 (4, OP)
C119.3 (2, OP&LP)
C119.4 (2, LP)

Fig. 7. Shoot K (A), Mg (B) and S (C) concentrations of cultivars Tapidor, Ningyou 7 and five $BC_4F_{2:3}$ lines generated with cultivar Tapidor as the recurrent parent and cultivar Ningyou 7 as the donor parent grown at LP in the agar system. Introgressed regions of cultivar Ningyou 7 in the QTL cluster Cl17.1 in these five lines are indicated in white in (D), and the physical positions of the five InDel markers are shown. All lines have five replicates except for the line 2292-3, which has three replicates. A significant difference between data for cultivar Tapidor and other genotypes is indicated by an asterisk (*$P < 0.05$, **$P < 0.01$) according to Student's *t*-test.

Figure 7.

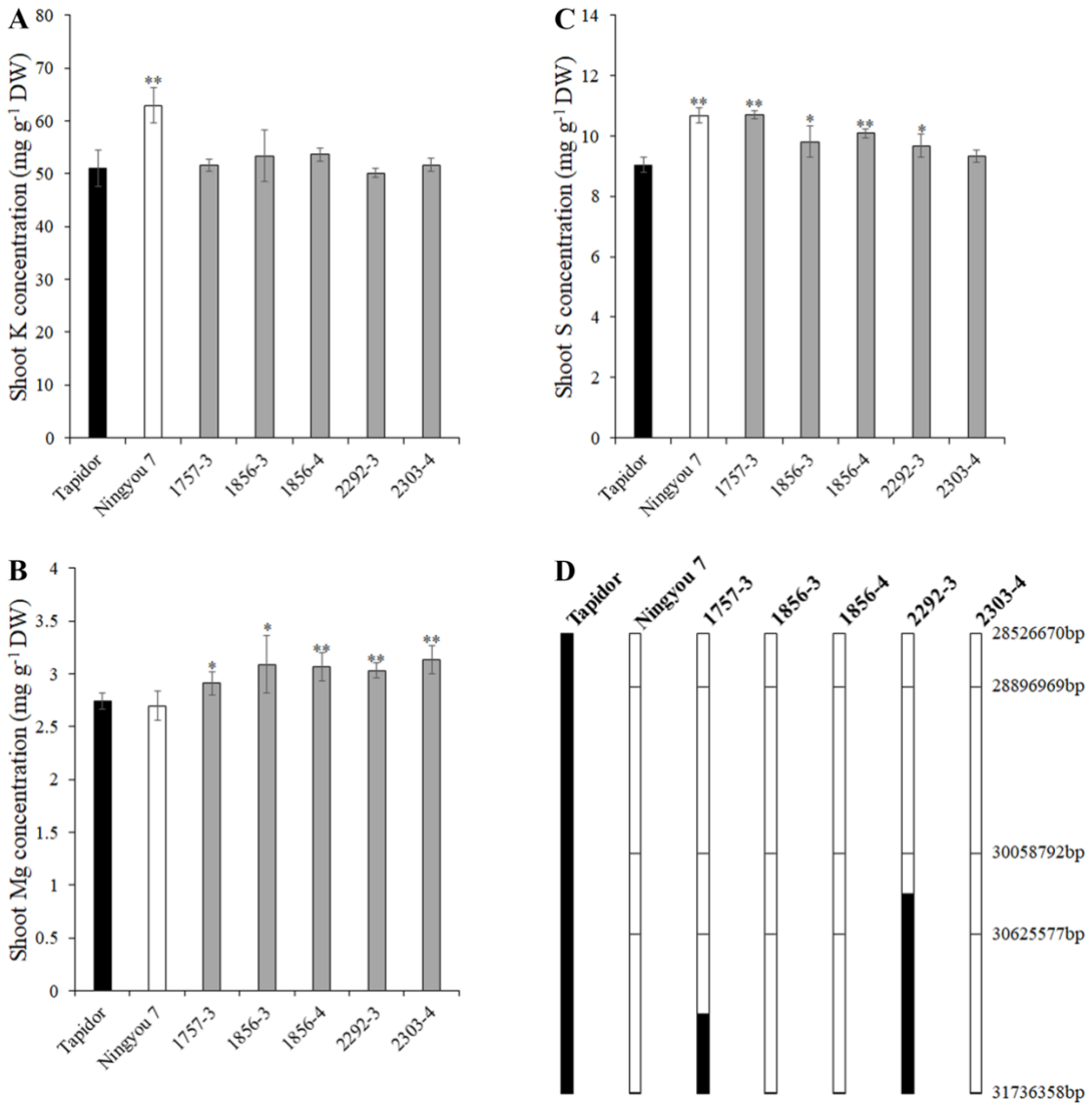
A
Shoot K concentration (mg g-1 DW)
Tapidor
Ningyou 7
1757-3
1856-3
1856-4
2292-3
2303-4
C
Shoot S concentration (mg g-1 DW)
B
Shoot Mg concentration (mg g-1 DW)
D
28526670bp
28896969bp
30058792bp
30625577bp
31736358bp

Table 1. Pearson's correlation coefficients among shoot concentrations and among root concentrations of eleven mineral elements in the *Bna*TNDH mapping population at an optimal (upper right triangle) and a low P supply (lower left triangle)

Correlation coefficients												
Shoot concentration		B	Ca	Cu	Fe	K	Mg	Mn	Na	P	S	Zn
	B	0.45**	0.11	0.33**	0.16*	0.39**	0.13	0.22**	0.25**	0.35**	-0.02	0.00
	Ca	0.36**	0.53**	0.14	-0.04	0.36**	0.37**	0.75**	0.49**	0.14	0.16*	0.45**
	Cu	-0.02	0.18*	0.18*	0.25**	0.09	0.11	0.08	0.11	0.14	0.02	0.12
	Fe	0.39**	0.42**	0.05	0.20*	-0.07	0.07	-0.10	0.11	-0.08	0.01	0.01
	K	0.47**	0.48**	0.15	0.25**	0.50**	-0.01	0.40**	0.26**	0.16*	0.05	0.18*
	Mg	0.11	0.40**	0.24**	0.02	0.44**	0.52**	0.27**	0.04	0.20**	0.28**	0.08
	Mn	0.45**	0.84**	0.07	0.37**	0.43**	0.27**	0.44**	0.19*	0.10	0.04	0.34**
	Na	0.58**	0.71**	0.19*	0.53**	0.57**	0.34**	0.56**	0.45**	0.17*	0.07	0.28**
	P	0.09	0.15	0.53**	-0.03	0.30**	0.54**	0.00	0.17*	0.16*	0.09	0.10
	S	0.14	0.13	0.15	-0.11	0.33**	0.28**	0.18*	0.12	0.15	0.69**	0.18*
	Zn	0.44**	0.62**	0.16*	0.66**	0.27**	0.05	0.62**	0.53*	0.05	0.11	-0.11
Root concentration		B	Ca	Cu	Fe	K	Mg	Mn	Na	P	S	Zn
	B	0.21**	0.38**	0.11	-0.02	0.10	0.07	0.46**	0.16*	0.02	-0.02	0.15
	Ca	0.44**	0.38**	-0.06	-0.14	0.17*	0.40**	0.70**	0.34**	0.08	-0.02	-0.01
	Cu	0.06	0.31**	0.05	0.14	-0.04	-0.06	-0.05	0.01	0.10	0.05	0.05
	Fe	-0.02	0.12	0.45**	0.32**	0.13	-0.14	0.06	0.06	0.18*	0.22**	0.04
	K	0.05	0.09	0.08	-0.02	0.56**	0.13	0.12	0.30**	0.08	0.17*	-0.09
	Mg	-0.08	0.17*	0.04	-0.03	0.22**	0.73**	0.22**	0.28**	0.33**	0.25**	0.17*
	Mn	0.43**	0.76**	0.14	0.19*	0.02	-0.02	0.34**	0.32**	0.01	0.04	0.06
	Na	0.29**	0.42**	0.11	0.11	0.31**	0.19*	0.35**	0.50**	-0.05	0.27**	0.11
	P	-0.06	-0.02	0.08	0.21**	0.28**	0.21**	0.03	-0.05	0.09	0.14	0.04
	S	0.01	0.10	0.06	0.13	0.42**	0.38**	-0.06	0.24**	0.09	0.58**	0.23**
	Zn	0.17*	0.46**	0.24**	0.14	0.15	-0.09	0.52**	0.17*	0.06	0.11	0.03

Grey values on the diagonal indicate the correlations between the two P treatments for each trait, *P<0.05, **P<0.01.

Table 2. Pearson's correlation coefficients among plant contents and among partitioning to the shoot of eleven mineral elements in the *Bna*TNDH mapping population at an optimal (upper right triangle) and a low P supply (lower left triangle)

		Correlation coefficients										
Plant content		B	Ca	Cu	Fe	K	Mg	Mn	Na	P	S	Zn
	B	0.67**	0.85**	0.68**	0.65**	0.94**	0.88**	0.88**	0.88**	0.89**	0.80**	0.72**
	Ca	0.84**	0.70**	0.66**	0.56**	0.90**	0.89**	0.95**	0.90**	0.84**	0.79**	0.81**
	Cu	0.47**	0.51**	0.27**	0.57**	0.66**	0.62**	0.62**	0.65**	0.62**	0.57**	0.59**
	Fe	0.54**	0.53**	0.40**	0.51**	0.64**	0.54**	0.59**	0.59**	0.57**	0.54**	0.58**
	K	0.93**	0.86**	0.53**	0.52**	0.66**	0.89**	0.93**	0.90**	0.88**	0.82**	0.77**
	Mg	0.81**	0.82**	0.50**	0.41**	0.90**	0.75**	0.87**	0.88**	0.88**	0.85**	0.73**
	Mn	0.89**	0.95**	0.49**	0.54**	0.90**	0.82**	0.69**	0.87**	0.85**	0.79**	0.81**
	Na	0.90**	0.91**	0.50**	0.59**	0.90**	0.81**	0.88**	0.70**	0.84**	0.80**	0.79**
	P	0.60**	0.57**	0.61**	0.28**	0.70**	0.75**	0.55**	0.59**	0.41**	0.78**	0.72**
	S	0.81**	0.74**	0.46**	0.38**	0.85**	0.80**	0.79**	0.75**	0.57**	0.76**	0.70**
	Zn	0.86**	0.87**	0.54**	0.62**	0.81**	0.68**	0.90**	0.84**	0.50**	0.71**	0.50**
Partitioning		B	Ca	Cu	Fe	K	Mg	Mn	Na	P	S	Zn
	B	0.56**	0.54**	0.30**	0.28**	0.52**	0.58**	0.60**	0.55**	0.40**	0.47**	0.61**
	Ca	0.58**	0.56**	0.06	0.23**	0.58**	0.58**	0.86**	0.59**	0.26**	0.48**	0.33**
	Cu	0.21**	0.32**	0.26**	0.15	0.05	0.13	0.04	0.10	0.26**	0.27**	0.20*
	Fe	0.32**	0.39**	0.33**	0.32**	0.19*	0.30**	0.24**	0.37**	0.28**	0.34**	0.37**
	K	0.51**	0.48**	0.16*	0.23**	0.69**	0.51**	0.57**	0.60**	0.31**	0.59**	0.36**
	Mg	0.47**	0.52**	0.21**	0.31**	0.58**	0.76**	0.50**	0.54**	0.48**	0.64**	0.56**
	Mn	0.62**	0.87**	0.25**	0.41**	0.49**	0.50**	0.52**	0.53**	0.25**	0.45**	0.38**
	Na	0.56**	0.71**	0.20**	0.32**	0.54**	0.57**	0.68**	0.65**	0.21**	0.50**	0.38**
	P	0.58**	0.43**	0.21**	0.39**	0.55**	0.54**	0.44**	0.41**	0.44**	0.54**	0.46**
	S	0.53**	0.46**	0.21**	0.35**	0.69**	0.64**	0.50**	0.46**	0.63**	0.78**	0.57**
	Zn	0.56**	0.69**	0.26**	0.37**	0.64**	0.59**	0.68**	0.59**	0.60**	0.64**	0.46**

Grey values on the diagonal indicate the correlations between the two P treatments for each trait, *P<0.05, **P<0.01.

1

Table 3. Significant QTLs associated with shoot and root concentrations, shoot, root and plant contents, and partitioning to the shoot of eleven mineral elements, shoot dry weight (SDW), root dry weight (RDW) and total dry weight (TDW) in the *Bna*TNDH population at an optimal (OP) and a low P supply (LP)

Trait	Mineral element	P treatment	QTL name	Chromosome	Position (cM)	LOD score	Confidence interval (cM)	Additive effect	R_2 (%)
Shoot concentration	B	OP	BconcOPS-A01	A01	48	4.73	47.5–49.5	1.617	13.6
		LP	BconcLPS-A03	A03	49	2.52	48.5–49.5	-1.332	6.8
	Ca	OP	CaconcOPS-A03	A03	45	2.63	44.5–45.5	-215.2	6.1
			CaconcOPS-A07	A07	89	6.28	88.5–89.5	311.9	15.0
		LP	CaconcLPS-A03	A03	38	4.16	35.5–42.5	-249.1	6.8
			CaconcLPS-A07	A07	88	10.39	87.5–88.5	378.9	18.0
			CaconcLPS-A09	A09	53	6.64	52.5–54.5	295.1	10.9
			CaconcLPS-C04	C04	63	2.82	61.5–68.5	-187.7	4.4
	Fe	LP	FeconcLPS-A02	A02	52	2.73	51.5–52.5	10.94	6.3
			FeconcLPS-A09	A09	137	3.68	136.5–139.0	12.59	8.6
			FeconcLPS-C06	C06	9	4.15	6.5–10.5	13.83	10.4
	K	OP	KconcOPS-A03	A03	45	8.14	44.5–45.5	-2201	3.6

		KconcOPS-A04	A04	37	3.54	36.5–37.5	1258	1.4
		KconcOPS-A09	A09	68	6.10	67.5–68.5	1679	2.4
		KconcOPS-C08a	C08	32	29.92	31.5–32.5	-4455	17.1
		KconcOPS-C08b	C08	34	21.69	33.5–36.5	3555	10.9
	LP	KconcLPS-A02	A02	73	3.98	72.5–73.5	-1536	5.2
		KconcLPS-A03	A03	47	3.91	46.5–47.5	-1490	5.1
		KconcLPS-A09	A09	116	3.43	115.5–116.5	1356	4.9
		KconcLPS-C06	C06	83	8.40	80.5–84.5	-2227	12.2
		KconcLPS-C07	C07	34	2.70	32.5–35.5	-1174	3.6
Mg	OP	MgconcOPS-A09	A09	81	2.61	78.5–82.5	77.90	6.3
		MgconcOPS-C07	C07	30	4.87	29.5–31.5	-109.7	11.9
	LP	MgconcLPS-A09	A09	92	4.91	91.5–93.5	130.3	9.8
		MgconcLPS-C07	C07	35	3.40	34.5–35.5	-109.6	6.6
Mn	OP	MnconcOPS-A04	A04	12	3.39	10.5–13.5	7.743	6.9
		MnconcOPS-A07	A07	89	3.13	88.5–89.5	7.712	6.9
		MnconcOPS-A08	A08	77	2.85	74.5–79.5	7.106	5.8
		MnconcOPS-C07	C07	89	4.12	88.5–90.5	-8.629	8.3
	LP	MnconcLPS-A07	A07	92	4.39	89.5–101.5	9.852	11.1

			MnconcLPS-A09	A09	53	4.23	52.5–54.5	9.538	10.4
	Na	LP	NaconcLPS-A09	A09	136	3.10	135.5–137.5	91.76	10.7
	P	OP	PconcOPS-A04	A04	36	3.76	31.5–36.5	437.6	8.5
			PconcOPS-C04	C04	39	4.34	36.5–39.5	-472.2	9.9
	S	OP	SconcOPS-A09	A09	11	12.76	8.5–16.5	-634.1	19.3
			SconcOPS-C02	C02	5	3.29	3.5–6.5	-300.2	4.6
			SconcOPS-C06	C06	16	6.59	15.5–18.5	-414.0	8.7
			SconcOPS-C07	C07	39	12.91	36.5–40.5	-627.2	19.3
		LP	SconcLPS-A09	A09	6	6.12	3.5–7.5	-583.3	12.7
			SconcLPS-C02	C02	46	3.17	44.5–47.5	-394.6	6.2
			SconcLPS-C07	C07	34	6.36	33.5–35.5	-588.7	13.3
Root concentration	B	OP	BconcOPR-A05	A05	12	4.83	11.5–14.5	-1.278	13.3
		LP	BconcLPR-A09a	A09	32	3.51	29.5–34.5	1.330	7.8
			BconcLPR-A09b	A09	128	3.36	124.5–128.5	1.164	6.3
	Cu	LP	CuconcLPR-A06	A06	85	2.71	84.5–85.5	0.962	7.3
	Fe	OP	FeconcOPR-C01	C01	47	3.14	45.5–48.5	126.4	11.4
	K	OP	KconcOPR-A06	A06	59	3.15	58.5–59.5	-1253	10.9
		LP	KconcLPR-A03	A03	92	3.63	91.5–92.5	1670	9.9
	Mg	OP	MgconcOPR-A07	A07	71	7.44	70.5–74.5	115.6	13.6

		MgconcOPR-C09	C09	46	3.10	45.5–47.5	-74.75	5.5
	LP	MgconcLPR-A03	A03	101	4.95	99.5–102.5	-91.12	9.2
		MgconcLPR-A04	A04	31	4.10	30.5–31.5	80.92	7.5
		MgconcLPR-A10	A10	49	3.54	48.5–49.5	-83.15	6.8
		MgconcLPR-C06	C06	76	2.52	75.5–76.5	-67.11	4.6
		MgconcLPR-C07	C07	67	3.79	65.5–67.5	79.20	6.9
Mn	OP	MnconcOPR-A08	A08	1	2.54	0–4.5	-4.041	6.6
Na	OP	NaconcOPR-A04	A04	31	2.55	30.5–31.5	61.66	4.8
		NaconcOPR-A09	A09	80	5.43	77.5–81.5	-95.59	11.6
		NaconcOPR-C03	C03	6	3.37	5.5–6.5	92.26	6.4
	LP	NaconcLPR-C03	C03	12	2.63	10.5–12.5	81.56	7.1
P	OP	PconcOPR-A09	A09	124	4.85	123.5–124.5	353.3	12.1
		PconcOPR-C04	C04	56	3.24	55.5–56.5	-282.5	7.8
		PconcOPR-C07	C07	2	2.55	0–2.5	249.1	6.1
S	OP	SconcOPR-A04	A04	37	10.98	36.5–37.5	476.9	19.2
		SconcOPR-A09	A09	9	4.22	8.5–15.5	-291.8	6.8
		SconcOPR-C01	C01	41	11.52	40.5–41.5	496.5	20.5
		SconcOPR-C09	C09	88	2.93	87.5–89.5	-233.1	4.6

		LP	SconcLPR-A04a	A04	27	14.09	26.5–27.5	700.3	23.1
			SconcLPR-A04b	A04	53	4.78	51.5–57.5	376.9	6.7
			SconcLPR-C01	C01	8	5.72	7.5–8.5	416.0	8.1
			SconcLPR-C05	C05	98	6.24	90.5–105.5	-483.6	11.1
	Zn	OP	ZnconcOPR-A03	A03	69	4.02	68.5–69.5	-18.83	9.2
			ZnconcOPR-A04a	A04	15	3.23	13.5–15.5	15.91	7.2
			ZnconcOPR-A04b	A04	65	2.73	64.5–67.5	14.66	6.1
			ZnconcOPR-C04	C04	3	2.93	2.5–3.5	-15.17	6.5
Shoot content	B	OP	BcontOPS-A03	A03	51	4.60	50.5–51.5	-0.026	12.5
		LP	BcontLPS-A03	A03	52	5.69	51.5–52.5	-0.025	14.8
			BcontLPS-A04	A04	5	3.95	4.5–5.5	-0.019	9.9
	Ca	OP	CacontOPS-A02	A02	75	3.99	74.5–75.5	-3.181	6.8
			CacontOPS-A03	A03	51	8.09	50.5–51.5	-4.456	14.5
			CacontOPS-A04	A04	3	2.57	2.5–4.5	-2.268	4.2
			CacontOPS-A07	A07	75	2.75	74.5–75.5	2.281	4.4
		LP	CacontLPS-A02	A02	112	4.22	99.5–120.0	-2.469	8.9
			CacontLPS-A03	A03	52	6.85	51.5–52.5	-3.066	11.7

		CacontLPS-A04	A04	5	5.71	4.5–5.5	-2.611	9.8
		CacontLPS-A07	A07	69	4.47	68.5–70.5	2.189	7.1
		CacontLPS-A09	A09	67	2.98	65.5–68.5	1.810	4.8
Cu	OP	CucontOPS-A03	A03	51	6.33	50.5–51.5	-0.004	16.6
Fe	LP	FecontLPS-A09	A09	136	4.95	135.5–136.5	0.108	12.8
K	OP	KcontOPS-A02	A02	75	5.86	74.5–75.5	-35.47	5.2
		KcontOPS-A03	A03	52	8.38	51.5–52.5	-41.48	7.6
		KcontOPS-A04	A04	3	3.20	2.5–4.5	-22.79	2.7
		KcontOPS-A09a	A09	68	14.67	66.5–68.5	51.86	14.2
		KcontOPS-A09b	A09	75	7.87	73.5–75.5	-36.06	6.9
	LP	KcontLPS-A02	A02	72	2.93	71.5–72.5	-19.88	6.4
		KcontLPS-A03	A03	52	4.78	51.5–52.5	-26.14	11.3
		KcontLPS-A04	A04	5	3.32	4.5–5.5	-19.93	7.5
Mg	OP	MgcontOPS-A02	A02	73	4.39	72.5–73.5	-1.556	8.1
		MgcontOPS-A03	A03	51	6.07	50.5–51.5	-1.810	11.6
		MgcontOPS-A04	A04	3	4.56	2.5–4.5	-1.443	8.3
	LP	MgcontLPS-A03	A03	59	5.12	58.5–59.5	-1.389	9.2
		MgcontLPS-A04	A04	5	6.06	4.5–5.5	-1.489	11.6

		MgcontLPS-A09	A09	74	2.91	73.5–74.5	1.028	5.7
Mn	OP	MncontOPS-A02	A02	75	2.97	74.5–75.5	-0.114	7.2
		MncontOPS-A03	A03	51	5.04	50.5–51.5	-0.142	12.2
	LP	MncontLPS-A03	A03	52	4.50	51.5–52.5	-0.117	10.3
		MncontLPS-A04	A04	5	3.91	4.5–5.5	-0.101	8.9
		MncontLPS-A07	A07	69	2.52	68.5–70.5	0.078	5.4
Na	OP	NacontOPS-A03	A03	51	3.79	50.5–51.5	-1.223	10.5
	LP	NacontLPS-A03	A03	52	4.80	51.5–52.5	-1.170	13.0
		NacontLPS-A04	A04	5	3.78	4.5–5.5	-0.963	10.2
		NacontLPS-A09	A09	132	2.68	130.5–132.5	0.775	6.8
P	OP	PcontOPS-A02	A02	79	46.12	78.5–79.5	-29.55	23.0
		PcontOPS-A03	A03	51	4.44	50.5–51.5	-6.583	1.1
		PcontOPS-A04	A04	2	3.85	1.5–2.5	-5.667	1.0
		PcontOPS-C04	C04	22	2.93	19.5–25.5	-4.843	0.7
	LP	PcontLPS-C09	C09	123	2.64	117.5–134.5	-2.403	7.1
S	OP	ScontOPS-A02	A02	73	3.37	72.5–73.5	-4.470	6.3
		ScontOPS-A03	A03	51	4.01	50.5–51.5	-4.815	7.8
		ScontOPS-A04	A04	3	5.42	2.5–4.5	-5.288	10.5
	LP	ScontLPS-A02	A02	54	3.33	53.5–54.5	-4.130	5.8

			ScontLPS-A03	A03	57	3.74	56.5–57.5	-4.567	6.5
			ScontLPS-A04	A04	5	7.63	4.5–5.5	-6.519	14.8
	Zn	OP	ZncontOPS-A03	A03	51	4.81	50.5–51.5	-0.084	13.3
		LP	ZncontLPS-A02	A02	106	2.66	92.5–120.0	-0.062	9.1
			ZncontLPS-A03	A03	52	3.57	51.5–52.5	-0.063	8.0
			ZncontLPS-A04	A04	5	3.51	4.5–5.5	-0.058	7.9
Root content	B	LP	BcontLPR-A03	A03	50	3.47	49.5–50.5	-0.003	13.7
	Ca	OP	CacontOPR-A03	A03	69	2.65	68.5–69.5	-0.333	7.8
		LP	CacontLPR-A03	A03	52	4.51	51.5–52.5	-0.398	11.7
	Cu	LP	CucontLPR-A05	A05	14	4.28	12.5–18.5	-0.001	10.8
			CucontLPR-A09	A09	71	2.81	70.5–71.5	-0.001	6.8
	K	LP	KcontLPR-A03	A03	52	2.79	51.5–52.5	-3.286	8.1
	Mg	OP	MgcontOPR-A03	A03	105	2.70	104.5–107.5	-0.154	8.0
		LP	MgcontLPR-A03	A03	85	4.79	84.5–85.5	-0.159	9.9
			MgcontLPR-A07	A07	53	4.23	52.5–53.5	0.145	8.2
			MgcontLPR-C04	C04	60	3.22	58.5–60.5	-0.127	6.4

Mn	OP	MncontOPR-A03	A03	69	2.54	68.5–69.5	-0.016	7.4
	LP	MncontLPR-A03	A03	52	4.03	51.5–52.5	-0.018	10.9
Na	LP	NacontLPR-A02	A02	107	4.12	96.5–120.0	-0.200	11.8
		NacontLPR-A03	A03	52	4.35	51.5–52.5	-0.178	8.1
P	OP	PcontOPR-A03	A03	78	4.85	76.5–81.5	-0.749	9.6
		PcontOPR-C04	C04	23	3.75	19.5–25.5	-0.652	7.4
		PcontOPR-C08	C08	69	3.77	66.5–69.5	-0.674	7.9
		PcontOPR-C09	C09	14	3.87	9.5–16.5	0.671	7.7
S	OP	ScontOPR-A03	A03	72	3.12	69.5–73.5	-0.987	8.7
	LP	ScontLPR-A03	A03	50	2.71	49.5–50.5	-0.828	8.7
		ScontLPR-A04	A04	38	5.45	37.5–38.5	0.994	14.5
		ScontLPR-C07	C07	84	2.52	83.5–84.5	-0.688	6.5
Zn	OP	ZncontOPR-A03	A03	69	6.81	68.5–69.5	-0.037	13.4
		ZncontOPR-A04	A04	65	3.49	64.5–67.5	0.025	6.5
		ZncontOPR-C04a	C04	6	2.86	3.5–9.5	-0.022	5.3
		ZncontOPR-C04b	C04	91	3.39	90.5–91.5	-0.024	6.2
		ZncontOPR-C09	C09	49	2.67	47.5–50.5	0.022	4.9
	LP	ZncontLPR-A03	A03	52	3.97	51.5–52.5	-0.018	10.4

			ZncontLPR-C04	C04	25	2.63	22.5–25.5	-0.013	6.6
Plant content	B	OP	BcontOPP-A03	A03	51	4.01	50.5–51.5	-0.027	11.8
		LP	BcontLPP-A03	A03	52	5.24	51.5–52.5	-0.027	13.8
			BcontLPP-A04	A04	9	3.83	8.5–9.5	-0.021	9.6
	Ca	OP	CacontOPP-A02	A02	73	4.06	72.5–73.5	-3.368	7.5
			CacontOPP-A03	A03	51	6.85	50.5–51.5	-4.380	13.6
			CacontOPP-C09	C09	49	3.11	47.5–50.5	2.724	5.7
		LP	CacontLPP-A02	A02	114	3.67	101.5–120.0	-2.603	8.3
			CacontLPP-A03	A03	52	6.67	51.5–52.5	-3.421	12.4
			CacontLPP-A04	A04	5	4.55	4.5–5.5	-2.647	8.6
			CacontLPP-A07	A07	69	4.40	68.5–70.5	2.469	7.6
	Cu	OP	CucontOPP-A03	A03	51	5.75	50.5–51.5	-0.005	16.0
		LP	CucontLPP-C05	C05	0	2.88	0–0.5	-0.002	8.4
	K	OP	KcontOPP-A02	A02	75	3.18	74.5–75.5	-32.69	8.8
			KcontOPP-A03	A03	51	5.17	50.5–51.5	-38.96	13.8
		LP	KcontLPP-A02	A02	72	2.77	71.5–72.5	-21.42	6.3
			KcontLPP-A03	A03	52	4.88	51.5–52.5	-29.28	12.0
			KcontLPP-A04	A04	5	2.73	4.5–5.5	-19.99	6.5

Mg	OP	MgcontOPP-A02	A02	73	4.09	72.5–73.5	-1.656	9.1
		MgcontOPP-A03	A03	51	4.63	50.5–51.5	-1.720	10.5
		MgcontOPP-A04	A04	9	4.21	8.5–9.5	-1.514	9.2
	LP	MgcontLPP-A04	A04	5	3.16	4.5–5.5	-1.291	12.4
Mn	OP	MncontOPP-A02	A02	75	3.15	74.5–75.5	-0.127	7.2
		MncontOPP-A03	A03	51	5.51	50.5–51.5	-0.160	12.7
		MncontOPP-C09	C09	48	3.12	47.5–49.5	0.113	6.8
	LP	MncontLPP-A03	A03	52	3.61	51.5–52.5	-0.120	11.3
		MncontLPP-A04	A04	5	2.58	4.5–5.5	-0.094	8.0
Na	OP	NacontOPP-A03	A03	51	6.31	50.5–51.5	-1.585	11.9
		NacontOPP-A04	A04	2	3.31	1.5–2.5	-1.063	5.9
		NacontOPP-C09	C09	48	2.93	47.5–49.5	1.000	5.1
	LP	NacontLPP-A02	A02	110	3.34	97.5–120.0	-1.188	10.8
		NacontLPP-A03	A03	52	5.19	51.5–52.5	-1.339	11.8

			NacontLPP-A04	A04	5	3.40	4.5–5.5	-1.015	7.8
			NacontLPP-A09	A09	139	2.54	135.5–139.0	0.830	5.3
	P	OP	PcontOPP-A03	A03	51	2.75	50.5–51.5	-6.400	8.4
		LP	PcontLPP-C09	C09	123	2.66	117.5–134.5	-2.567	7.2
	S	OP	ScontOPP-A02	A02	73	4.95	72.5–73.5	-6.198	11.2
			ScontOPP-A03	A03	56	3.24	55.5–56.5	-4.845	7.4
			ScontOPP-A04	A04	8	3.71	7.5–8.5	-4.869	8.3
			ScontOPP-C07	C07	50	2.72	48.5–50.5	-4.318	6.1
		LP	ScontLPP-A02	A02	54	3.31	53.5–54.5	-4.601	6.4
			ScontLPP-A03	A03	57	3.75	56.5–57.5	-5.110	7.3
			ScontLPP-A04	A04	5	5.58	4.5–5.5	-6.186	11.9
			ScontLPP-C07	C07	40	2.90	38.5–41.5	-4.381	5.8
	Zn	OP	ZncontOPP-A03	A03	69	6.35	68.5–69.5	-0.121	14.9
		LP	ZncontLPP-A02	A02	107	2.59	93.5–120.0	-0.073	8.6
			ZncontLPP-A03	A03	50	3.23	49.5–50.5	-0.072	7.0
Partitioning	B	OP	BpartOP-C04	C04	91	2.55	90.5–91.5	0.447	11.1
		LP	BpartLP-A04	A04	5	4.15	4.5–5.5	-0.532	8.9
			BpartLP-C04	C04	60	3.21	58.5–60.5	0.475	7.2
			BpartLP-C07	C07	93	3.71	92.5–93.0	0.506	8.1
	Ca	OP	CapartOP-A05	A05	89	3.07	88.5–89.5	0.383	7.0
			CapartOP-C02	C02	3	3.85	1.5–5.5	0.420	8.5
			CapartOP-C03	C03	120	5.89	118.5–120.5	0.521	12.9
			CapartOP-C05	C05	83	2.70	81.5–88.5	-0.349	5.8
			CapartOP-C09	C09	117	3.14	116.5–117.5	-0.373	6.7

	LP	CapartLP-A07	A07	88	3.97	87.5–88.5	0.576	9.6
		CapartLP-A09	A09	61	4.49	60.5–61.5	0.617	11.0
		CapartLP-C09	C09	117	3.36	116.5–117.5	-0.531	8.1
Cu	LP	CupartLP-A05	A05	16	2.82	12.5–18.5	2.145	7.0
		CupartLP-A09	A09	91	2.74	90.5–92.5	2.124	6.8
Fe	OP	FepartOP-A01	A01	84	4.18	82.5–84.5	1.121	9.7
		FepartOP-A04	A04	14	2.60	13.5–15.5	-0.873	6.1
		FepartOP-C03	C03	85	4.77	83.5–85.5	1.184	11.2
		FepartOP-C09	C09	117	2.75	116.5–117.5	-0.889	6.3
K	OP	KpartOP-A02	A02	81	5.19	80.5–81.5	-0.744	7.5
		KpartOP-A05	A05	40	5.88	37.5–40.5	-0.730	8.4
		KpartOP-A09	A09	40	2.89	38.5–42.5	0.538	4.5
		KpartOP-C03	C03	137	6.99	133.5–142.0	0.818	10.6
	LP	KpartLP-A04	A04	8	3.86	7.5–8.5	-0.809	11.4
Mg	OP	MgpartOP-A07	A07	69	3.20	68.5–70.5	-0.468	6.4
		MgpartOP-C04	C04	54	4.35	50.5–54.5	0.551	8.9
	LP	MgpartLP-A07	A07	53	3.58	52.5–53.5	-0.551	6.5
		MgpartLP-C04	C04	55	5.12	54.5–55.5	0.665	9.6
Mn	OP	MnpartOP-A09	A09	79	4.50	77.5–81.5	0.515	9.7
		MnpartOP-C02	C02	16	2.98	15.5–19.5	0.411	6.2
		MnpartOP-C03	C03	120	3.72	118.5–120.5	0.463	7.7
		MnpartOP-C05	C05	91	4.87	90.5–102.5	-0.537	10.4
Na	OP	NapartOP-A04	A04	58	5.31	54.5–58.5	-0.832	14.5
		NapartOP-A09	A09	54	4.39	52.5–54.5	0.750	11.7
	LP	NapartLP-A04	A04	31	7.29	30.5–31.5	-0.833	10.9
		NapartLP-A05	A05	12	2.85	10.5–12.5	0.506	4.0
		NapartLP-A09	A09	121	3.72	120.5–122.5	0.584	5.3
		NapartLP-C03	C03	12	4.16	10.5–12.5	-0.710	6.1
P	OP	PpartOP-A03	A03	76	2.92	75.5–76.5	0.341	7.6

			PpartOP-C04	C04	91	3.99	90.5–91.5	0.393	10.3
	S	OP	SpartOP-A04	A04	8	11.12	7.5–8.5	-1.253	20.8
			SpartOP-A09	A09	45	3.46	44.5–45.5	0.650	5.7
			SpartOP-A10	A10	74	5.02	72.5–75.0	0.893	8.3
			SpartOP-C02	C02	45	3.16	43.5–46.5	-0.628	5.3
		LP	SpartLP-A04	A04	7	11.63	6.5–7.5	-1.464	24.9
			SpartLP-A05	A05	112	2.75	110.5–112.0	0.658	5.1
			SpartLP-C09	C09	14	4.45	10.5–17.5	-0.852	8.5
	Zn	OP	ZnpartOP-A03	A03	69	4.83	68.5–69.5	1.286	8.7
			ZnpartOP-A04a	A04	8	6.19	7.5–8.5	-1.424	11.6
			ZnpartOP-A04b	A04	65	6.33	64.5–66.5	-1.423	11.7
			ZnpartOP-C04a	C04	5	4.75	3.5–7.5	1.256	9.1
			ZnpartOP-C04b	C04	91	3.58	90.5–91.5	1.050	6.3
		LP	ZnpartLP-A04	A04	13	8.69	11.5–13.5	-1.134	18.7
			ZnpartLP-C08	C08	31	3.41	27.5–31.5	-0.705	7.2
			ZnpartLP-C09	C09	127	3.14	125.5–141.0	-0.668	6.5
Shoot dry weight		OP	SDWOP–A02	A02	75	2.98	74.5–75.5	-0.374	6.7
			SDWOP–A03	A03	51	4.81	50.5–51.5	-0.451	10.7
			SDWOP–A04	A04	3	4.06	2.5–3.5	-0.389	8.9
		LP	SDWLP–A02	A02	103	2.63	86.5–117.5	-0.328	8.3
			SDWLP–A03	A03	52	3.31	51.5–52.5	-0.324	6.8
			SDWLP–A04	A04	9	4.73	8.5–9.5	-0.354	9.7
Root dry weight		LP	RDWLP–A03	A03	52	3.01	51.5–52.5	-0.070	8.5
Total dry weight		OP	TDWOP-A02	A02	73	2.89	72.5–73.5	-0.420	6.0
			TDWOP-A03	A03	51	4.79	50.5–51.5	-0.536	10.3
			TDWOP-A04	A04	3	3.45	2.5–4.5	-0.425	7.3
		LP	TDWLP-A02	A02	72	2.53	71.5–72.5	-0.324	4.8
			TDWLP-A03	A03	52	4.94	51.5–52.5	-0.465	10.2
			TDWLP-A04	A04	9	4.25	8.5–9.5	-0.388	8.4

Note: each QTL for shoot and root concentrations of eleven mineral elements was denominated as "mineral element + conc (abbreviation of concentration) + P treatment + S (abbreviation of shoot) or R (abbreviation of root) + chromosome + the serial letter". Each QTL for shoot, root and plant contents of eleven mineral elements was denominated as "mineral element + cont (abbreviation of content) + P treatment + S (abbreviation of shoot) or R (abbreviation of root) or P (abbreviation of plant) + chromosome + the serial letter". Each QTL for partitioning of eleven mineral elements was denominated as "mineral element + part (abbreviation of partitioning) + P treatment + chromosome + the serial letter". Each QTL for biomass traits was denominated as "trait + P treatment + chromosome". A positive additive effect indicates a positive contribution of the Tapidor allele to the trait value, and a negative additive effect indicates a positive contribution of the Ningyou 7 allele to the trait value. R_2, the explained phenotypic variation.

Table 4. Epistatic loci for shoot and root concentrations, shoot, root and plant contents, and partitioning to the shoot of eleven mineral elements, and total dry weight in the *Bna*TNDH population at an optimal (OP) and a low P supply (LP)

Trait	Mineral element	P treatment	Chromosome1	Position 1 (cM)	LeftMarker1	RightMarker1	Chromosome2	Position 2 (cM)	LeftMarker2	RightMarker2	LOD score	R_2 (%)	Add1	Add2	Add by Add
Shoot concentration	Cu	OP	A10	35	C10M37	C10M38	C04	40	C14M26	C14M27	5.03	13.6	0.104	-0.201	-0.456
			A09	45	C9M24	C9M25	C09	70	C19M43	C19M44	5.26	15.0	-0.185	0.088	-0.452
	Fe	OP	A02	25	C2M18	C2M19	A05	30	C5M21	C5M22	5.32	11.3	0.284	0.336	5.171
			A06	20	C6M15	C6M16	A06	35	C6M31	C6M32	5.26	14.5	7.053	-5.832	-7.992
			A05	35	C5M27	C5M28	A07	70	C7M94	C7M95	5.12	11.0	0.387	-1.363	-5.010
			C04	40	C14M26	C14M27	C07	0	C17M1	C17M2	5.54	11.9	0.805	1.204	5.262
		LP	A02	70	C2M80	C2M81	A02	85	C2M104	C2M105	5.13	17.9	3.384	-8.349	-19.18
	K	LP	A01	15	C1M6	C1M7	A09	30	C9M17	C9M18	5.37	10.5	-305.9	-98.64	-1588

	P	OP	A08	30	C8M22	C8M23	A09	75	C9M71	C9M72	6.26	16.1	-77.59	100.9	-529.0
	S	LP	A06	30	C6M24	C6M25	C06	95	C16M74	C16M75	5.00	8.0	-27.88	47.10	-494.7
	Zn	LP	A02	70	C2M80	C2M81	A02	95	C2M106	C2M107	7.39	17.0	11.02	-11.09	-14.18
Root concentration	B	LP	A03	130	C3M155	C3M156	A06	15	C6M6	C6M7	5.25	13.1	-0.310	-0.119	1.428
	Mg	LP	A02	80	C2M100	C2M101	C07	0	C17M1	C17M2	6.03	11.2	10.85	-69.45	-96.72
			A05	0	C5M1	C5M2	C09	60	C19M31	C19M32	5.51	10.7	7.897	-27.76	90.33
	Mn	OP	A04	5	C4M7	C4M8	A08	0	C8M1	C8M2	5.31	24.4	0.456	-4.338	5.191
	Zn	OP	A03	60	C3M54	C3M55	A10	45	C10M54	C10M55	5.01	23.0	11.13	-4.230	21.96
		LP	A06	115	C6M137	C6M138	A06	120	C6M137	C6M138	7.32	6.8	-22.19	20.13	-22.93

Shoot content	Cu	LP	A05	70	C5M72	C5M73	C05	50	C15M25	C15M26	5.13	20.7	-0.001	-0.002	0.003
	K	LP	A08	20	C8M10	C8M11	C05	70	C15M44	C15M45	5.09	15.8	-9.759	-2.021	-23.88
	Mg	LP	C06	70	C16M54	C16M55	C07	90	C17M77	C17M78	5.54	16.2	-0.094	0.316	1.348
	Mn	OP	A06	65	C6M81	C6M82	A10	10	C10M5	C10M6	5.12	12.3	0.016	0.010	-0.126
		LP	A01	40	C1M70	C1M71	C05	110	C15M54	C15M55	6.32	17.4	0.003	-0.006	0.124
	S	OP	A05	25	C5M16	C5M17	C04	25	C14M13	C14M14	5.35	18.6	-2.448	-0.175	-4.998
			A09	120	C9M132	C9M133	C08	50	C18M37	C18M38	5.37	15.7	-1.288	-0.771	4.806
	Zn	LP	C05	40	C15M19	C15M20	C05	70	C15M44	C15M45	5.31	17.4	-0.045	0.023	-0.080
Root content	B	OP	A10	40	C10M46	C10M47	A10	45	C10M54	C10M55	5.59	12.0	-0.012	0.013	-0.012
			C09	10	C19M3	C19M4	C09	15	C19M4	C19M5	5.45	13.4	-0.011	0.013	-0.013

	LP	A03	0	C3M1	C3M2	A08	5	C8M2	C8M3	5.05	14.4	0.001	0.000	0.004
Cu	OP	A03	40	C3M12	C3M13	A03	45	C3M15	C3M16	5.22	13.6	0.003	-0.003	-0.003
K	OP	A10	40	C10M46	C10M47	A10	45	C10M54	C10M55	5.94	7.6	-17.14	16.64	-15.09
		C03	75	C13M73	C13M74	C03	80	C13M74	C13M75	5.06	8.1	-13.40	14.50	-18.26
		C05	35	C15M18	C15M19	C05	40	C15M19	C15M20	5.36	8.8	-12.53	9.906	-19.37
		C09	10	C19M3	C19M4	C09	15	C19M4	C19M5	6.44	8.8	-13.73	16.80	-16.69
Mn	OP	A10	40	C10M46	C10M47	A10	45	C10M54	C10M55	5.32	11.1	-0.056	0.055	-0.053
		C09	10	C19M3	C19M4	C09	15	C19M4	C19M5	5.57	13.2	-0.045	0.055	-0.058
Na	OP	C07	50	C17M37	C17M38	C08	50	C18M37	C18M38	5.05	16.4	-0.122	-0.143	0.247
S	OP	A02	30	C2M20	C2M21	A02	45	C2M26	C2M27	5.14	11.7	-0.857	1.139	-1.945

	Zn	OP	A05	35	C5M27	C5M28	A05	40	C5M32	C5M33	6.54	7.4	0.086	-0.088	-0.106
			C09	10	C19M3	C19M4	C09	15	C19M4	C19M5	5.67	8.1	-0.082	0.085	-0.110
Plant content	B	OP	A01	25	C1M23	C1M24	A05	110	C5M103	C5M104	5.08	19.0	0.008	-0.001	0.027
	Fe	LP	C03	140	C13M126	C13M127	C06	75	C16M59	C16M60	5.26	15.6	-0.170	0.071	-0.351
	K	LP	A03	0	C3M1	C3M2	A08	20	C8M10	C8M11	5.10	16.5	-1.978	-8.171	26.65
			A08	20	C8M10	C8M11	C05	70	C15M44	C15M45	5.14	17.4	-10.22	-2.131	-26.73
	Mn	LP	A03	0	C3M1	C3M2	A08	5	C8M2	C8M3	5.76	15.8	0.004	-0.022	0.134
			A01	40	C1M70	C1M71	C05	115	C15M55	C15M56	5.04	13.1	-0.010	0.011	0.123
	Na	LP	A08	20	C8M10	C8M11	C05	70	C15M44	C15M45	5.74	17.0	-0.320	-0.136	-1.261

	Zn	LP	C05	35	C15M18	C15M19	C05	70	C15M44	C15M45	5.38	15.2	-0.055	0.024	-0.092
Partitioning	Mg	OP	C08	55	C18M46	C18M47	C08	100	C18M99	C18M100	5.29	11.3	0.299	0.030	0.618
	Mn	LP	A06	100	C6M128	C6M129	C05	40	C15M19	C15M20	5.41	13.8	0.039	0.198	-0.685
	Na	OP	A01	0	C1M1	C1M2	A05	10	C5M3	C5M4	6.05	11.7	-0.013	0.111	-0.814
			A06	95	C6M124	C6M125	A06	120	C6M137	C6M138	5.16	11.8	0.128	-0.548	0.930
	Zn	OP	A03	70	C3M72	C3M73	A10	55	C10M67	C10M68	5.25	18.1	-0.827	0.884	-1.483
Total dry weight		OP	A06	25	C6M19	C6M20	C03	90	C13M80	C13M81	5.10	7.8	-0.063	0.115	-0.479
		LP	A08	30	C8M22	C8M23	C03	5	C13M4	C13M5	5.43	11.0	-0.476	-0.237	0.518

Note: a positive value of Add by Add indicates that two loci genotypes being the same as those in parent Tapidor (or Ningyou 7) take the positive effects, while the two-loci recombinants take the negative effects. The case of negative values is just the opposite. R_2, the explained phenotypic variation.

1

2